Liver Cancer

Research Article

Liver Cancer 2024;13:285–305
DOI: 10.1159/000533818

Received: May 8, 2023
Accepted: August 22, 2023
Published online: October 9, 2023

Two Distinct Characteristics of Immune Microenvironment in Human Hepatocellular Carcinoma with Wnt/β-Catenin Mutations

Tomoko Aoki[a] Naoshi Nishida[a] Yutaka Kurebayashi[b] Kazuko Sakai[c] Masahiro Morita[a] Hirokazu Chishina[a] Masahiro Takita[a] Satoru Hagiwara[a] Hiroshi Ida[a] Kazuomi Ueshima[a] Yasunori Minami[a] Masakatsu Tsurusaki[d] Takuya Nakai[e] Michiie Sakamoto[b] Kazuto Nishio[c] Masatoshi Kudo[a]

[a]Department of Gastroenterology and Hepatology, Kindai University Faculty of Medicine, Osakasayama, Japan; [b]Department of Pathology, Keio University School of Medicine, Tokyo, Japan; [c]Department of Genome Biology, Kindai University Faculty of Medicine, Osaka, Japan; [d]Department of Radiology, Kindai University Faculty of Medicine, Osakasayama, Japan; [e]Department of Surgery, Faculty of Medicine, Kindai University, Osaka, Japan

Keywords
Hepatocellular carcinoma · Wnt/β-catenin mutation · Tumor microenvironment · Inflamed tumors · Non-inflamed tumors

Abstract

Introduction: Immunotherapy is becoming a promising approach for unresectable-hepatocellular carcinoma (HCC); the anti-tumor response is affected by the tumor microenvironment (TME). Although Wnt/β-catenin mutations are reported to cause non-inflamed phenotype, their role on TME remains controversial. We aimed to clarify the heterogeneity of immunophenotype in HCC with Wnt/β-catenin mutations. ***Methods:*** This study includes 152 resected HCCs; mutations in the *catenin beta-1*, *adenomatous polyposis coli,* or *AXIN1*, or *AXIN2* genes were defined as Wnt/β-catenin mutations. With hierarchical cluster analyses, TME was classified into inflamed or non-inflamed classes based on the gene expressions associated with T-cell activation. Expression profiles of molecules related to cell differentiation and biliary-stem cell markers were compared between the TME classes to investigate whether differences in tumor traits were associated with TME. ***Results:*** Forty of 152 (26.3%) HCCs carried the Wnt/β-catenin mutations. Of these, 33 were classified as non-inflamed (33/40, 82.5%) and 7 as inflamed (7/40, 17.5%). Non-inflamed class was characterized by low number of CD3+, CD4+, and CD8+ cells on immunostaining, and high mRNA expressions of *AXIN2 and GLUL,* which are involved in the canonical Wnt/β-catenin signaling and hepatocyte differentiation, respectively. Non-inflamed tumors showed higher enhancement on the hepatobiliary-phase of gadolinium-ethoxybenzyl-diethylenetriamine (Gd-EOB-DTPA)-enhanced magnetic resonance imaging (MRI) compared to inflamed tumors. HCCs classified as inflamed class are revealed to have high numbers of CD3+, CD4+, and CD8+ tumor infiltrating lymphocytes on immunostaining. This class is associated with increased expression of anti-epithelial cell adhesion molecule and FOXM1 accompanied by upregulation of genes related to interferon-gamma signaling, dendritic cell migration, regulatory T cells, and myeloid-derived suppressor cell activation and recognized as low enhancement nodule

Tomoko Aoki and Naoshi Nishida contributed equally to this manuscript.

karger@karger.com
www.karger.com/lic

Correspondence to:
Naoshi Nishida, naoshi@med.kindai.ac.jp

on Gd-EOB-DTPA-enhanced MRI. ***Conclusion:*** Heterogeneity of tumor traits and TME was observed in HCC with Wnt/β-catenin mutation. The potential was indicated that tumor traits and TME are determined not only by the activation of the *HNF4A* but also by *FOXM1*, both of which are downstream transcription factor of the Wnt/β-catenin signaling pathway.

Introduction

Patients with recurrence of hepatocellular carcinoma (HCC) after curative therapies, such as radiofrequency ablation and surgical resection [1], eventually progress to an advanced stage of the disease; appropriate management of these patients is critical for long-term survival. Immune-mediated therapies including treatment with immune checkpoint inhibitors (ICIs) are a key strategy for the treatment of unresectable HCC; the antitumor effect of the agents should be attributed to the immune conditions in the tumor microenvironment (TME) [2]. Refractory non-inflamed tumors represent a major challenge to immune-mediated therapies for HCC. Blockade of infiltration of $CD8^+$ T cells into tumors has been partly attributed to the emergence of Wnt/β-catenin activating mutations [3–5], with activation of this pathway leading to a reduced recruitment of $CD103^+$ dendritic cells (DCs) caused by the downregulation of chemokine (c-c motif) ligand 5 (CCL5) [5, 6]. HCC with Wnt/β-catenin mutation has been shown to be refractory to ICI, both for anti-programmed cell death protein 1 (PD-1)/programmed death-ligand 1 (PD-L1) antibody monotherapy [7, 8] and immune-combination therapies such as atezolizumab plus bevacizumab [9].

Hepatocyte nuclear factor (HNF) 4α, which is involved in organ-specific differentiation and also acts as a tumor suppressor gene, is one of the target genes of the Wnt/β-catenin signaling pathway [10, 11]. Therefore, HCCs with Wnt/β-catenin mutations generally show a differentiated phenotype with less vascular invasion and extrahepatic metastasis, increased expression of molecules characteristic for mature hepatocytes including the bile acid transporter organic anion transporting polypeptide (OATP)1B3 [12]. This HCC type exhibits higher enhancement on the hepatobiliary phase of gadolinium-ethoxybenzyl-diethylenetriamine (Gd-EOB-DTPA)-enhanced magnetic resonance imaging (MRI) [13–15].

However, recently, it has been reported that a subset of HCCs with Wnt/β-catenin activating mutations may also show aggressive phenotypes [16]; another study identified a subgroup that responds to immunotherapy [17]. Some reports have suggested a dual aspect of Wnt/β-catenin mutated HCC in terms of the tumor behavior and anti-tumor response to ICIs [16, 18]. This indicates that the phenotypic heterogeneity of Wnt/β-catenin mutated HCC may be mainly attributed to differences among master regulators on the Wnt/β-catenin signaling that leads to the expression of immune gene sets characteristic for immunological TME. In this context, we specifically focused on the major master regulators for the phenotypic heterogeneity for this type of HCC, such as HNF4α and forkhead box (FOX) M1 because variations in tumor differentiation and aggressiveness may affect the TME through the different amount of tumor-related antigens [18]. In this context, we classified the Wnt/β-catenin mutated HCCs based on the transcriptome data for an accurate characterization of the immune microenvironment and compared the phenotypic differences of HCC in each class.

Materials and Methods

Patients

This is single-institution retrospective cohort study enrolled 152 patients with Child-Pugh class A liver function [19] who underwent curative surgical resection of HCC at the Kindai University Hospital between December 2003 and July 2014. The diagnosis of HCC was made based on radiological findings as recommended by the guidelines of the American Association for the Study of Liver Diseases [20]. The inclusion criteria were as follows: patients with performance status defined by the Eastern Cooperative Oncology Group [21] of zero or 1; patients who met the Makuuchi criteria [22, 23] and could tolerate hepatic resection; patients who met tumor conditions with no extrahepatic spread including lymph node metastases.

We analyzed the background of these 152 patients and prognosis, including recurrence-free survival (RFS) and overall survival (OS). The following blood and biochemical laboratory values were collected from the medical records within 1 month prior to liver resection: white blood cell count, lymphocyte count, neutrophil-to-lymphocyte ratio, red blood cell distribution width, platelet count, C-reactive protein, hyaluronic acid, prothrombin time – international normalized ratio, serum albumin, total bilirubin, aspartate aminotransferase, alanine aminotransferase, gamma glutamate transferase, lactate dehydrogenase, corrected calcium, alpha-fetoprotein, and des-γ-carboxyprothrombin.

This study was conducted in accordance with the Declaration of Helsinki and was approved by the Institutional Review Board of the Kindai University Hospital (approval No. #31-145). The requirement for informed consent for the academic use of archived samples for this noninvasive retrospective study was waived with an opt-out approach in the event of publication of the research plan under the Act on the Protection of Personal Information in Japan.

DNA and RNA Analysis Using Next-Generation Sequencers

DNA and RNA were extracted from archived fresh frozen samples. The tumor tissues were frozen immediately after surgical removal and stored at 80jC until DNA and RNA isolation. AllPrep DNA/RNA formalin-fixed paraffin-embedded (FFPE) kit (QIAGEN; Venlo, the Netherlands) was used to extract DNA and RNA from samples. The Ion AmpliSeqTM Comprehensive Cancer Panel (Illumina®; San Diego, CA, USA), which targets somatic mutations across 409 cancer-related genes was applied to examine the gene mutations in tumor tissue. The Wnt/β-catenin activating mutations were defined as mutations of the *catenin beta-1* (*CTNNB1*), *adenomatous polyposis coli* (*APC*), *AXIN1*, or *AXIN2* genes in tumor tissues. After non-synonymous mutations were selected, the low-quality sequences were excluded. Single nucleotide polymorphisms listed in the Human Genome Variation Database (HGVD) version 2.3 were also filtered out. However, mutations that were registered in the reference database as single nucleotide polymorphisms but showed prominent increase of clonality in tumor tissues compared to non-tumor tissues were considered as oncogenic alterations. Allele reads were counted, and tissues contained clonally expanded mutant cells if the absolute number of corresponding mutant alleles was ≥20 leads. We also used prediction algorithms to determine the significance of missense mutations in carcinogenesis: the sorting intolerant from tolerant and polymorphism phenotyping v2 functional prediction algorithm [24, 25].

For library preparation for transcriptome analysis, Ion AmpliSeq Transcriptome Human Gene Expression Kit (Thermo Fisher Scientific, Inc.; Waltham, MA, USA) was used for next-generation sequencing with following the manufacturer's protocol. Sequencing was performed using the Ion 550 Kit and the Ion S5TM XL System (Thermo Fisher Scientific, Inc.). To classify the TME status, we performed hierarchical clustering analysis and generated heat maps using the mRNA expression related to tumor-infiltrating CT8+ T lymphocytes (TILs), immune escape, DC activation, natural killer cell activation, interferon gamma (IFN-γ) signaling, myeloid-derived suppressor cells (MDSCs), regulatory T (Treg) cells, and antigen presentation based on a previous report (shown in online suppl. Table 1; for all online suppl. material, see https://doi.org/10.1159/000533818) [26–28]. For the characterization of HCCs belonging to each subgroup of TME determined by the clustering analysis, we compared gene expression levels for *CTNNB1, AXIN1, AXIN2, and APC* as a canonical Wnt/β-catenin activating signaling. We also compared the expression levels of several genes as follows for the accurate characterization of immune subgroups; *glutamate-ammonia ligase (GLUL), Solute Carrier Organic Anion Transporter (SLCO) 1B3*, and gene card of a bile acid transporter as differentiation markers; *SNAI1, SNAI2, SNAI3, EST, TWIST1*, and *VIM* as epithelial-mesenchymal transition (EMT)-related genes; *vascular endothelial growth factor (VEGF), fibroblast growth factor receptor (FGFR), Transforming Growth Factor-β1 (TGFB1), IFN-γ, NOTCH, CC chemokine ligand (CCL), chemokine (C-X-C motif) ligand (CXCL), and matrix metalloproteinase (MMP) as* representatives of immune-related signaling pathways.

Immunohistochemistry

FFPE samples of HCC tissue obtained from liver resection were examined to confirm the histology of HCC by pathologists specializing in hepatology (Y.K. with 10 years, and M.S. with 37 years of experience in pathological diagnosis of liver tumor). Immunohistochemistry (IHC) was used to determine the nuclear deposition of β-catenin, expression of glutamine synthetase (GS) as a marker of canonical Wnt/β-catenin signaling and hepatocyte differentiation; FOXM1 as a marker of downstream molecule relate to cell proliferation in Wnt/β-catenin signaling; CK19, SALL4, and epithelial cell adhesion molecule (EpCAM) as markers of the biliary stem cells. Expression of TILs and expression of PD-1, PD-L1, T-cell immunoglobulin mucin (TIM)-3, and lymphocyte-activation gene (LAG)-3 were also examined with IHC.

Strong diffuse staining of GS was defined as positive, and for β-catenin evaluation, nuclear staining of ≥5% of tumor cells was defined as positive [29]. To evaluate CK19 expression, we assessed membranous and/or cytoplasmic expression of tumor cells; positivity was defined as strong CK19 staining in more than 1–5% of tumor cells. For SALL4, positivity was defined as the presence of a nuclear-reactive spreading pattern in more than 1–5% of tumor cells. For EpCAM, membranous staining in greater than or equal to 1–5% of tumor cells was defined as positive [29]. PD-1, LAG-3, or TIM-3 expression was determined to be positive when the T-lymphocyte membrane showed yellow, brown, or dark brown granules [8, 30]. The number of PD-L1 positive cells in the tumor and tumor infiltrating cells were summed to calculate the combined positive score (CPS), which was determined as the number of PD-L1 positive cells divided by the total number of viable tumor cells × 100 [31]. Details of the IHC conditions are set out in online supplementary Table 2.

MRI Protocol

Gd-EOB-DTPA-enhanced MRI was performed on a 3T scanner (Intera Achieva 3T, Philips Healthcare, Best, Netherlands) or 1.5T scanner (1.5T Signa HDxt, GE Healthcare, Milwaukee, WI, USA) using a superconducting magnet system with an 8-channel body phased-array coil. Gadoxetate (Primovist: Bayer Schering Pharma, Osaka, Japan) was administered intravenously at a rate of 0.025 mmol per kg body weight at 2.0 mL/s, followed by a 20-mL saline flush. Dynamic images using fat-suppressed T1-weighted gradient echo images were obtained before (pre-contrast), 14–30 s (arterial phase), 70 s, 3 min, and 20 min (hepatobiliary phase images) after the injection of gadoxetic acid.

In the present study, the radiologist (M.T. with 19 years of experience in abdominal radiology, particularly liver imaging) calculated the relative enhancement of nodules compared with that of the liver parenchyma as follows [13, 32]: the relative intensity ratio (RIR) = SInod/SIpar, where SInod is the SI from the nodule and SIpar is that from the liver parenchyma; the relative enhancement ratio (RER) was calculated as RIRHBP/RIRpre, where RIRHBP is RIR in the hepatobiliary phase images and RIRpre is the RIR before the contrast enhancement.

Statistical Analyses

First, principal component analysis was performed in all 152 HCCs by gene expression levels of CD8+ T cells, IFN-γ signal, and TGFB1 to confirm the distribution of inflammatory and non-inflammatory classes, as reported by Sia et al. [33]. We next performed hierarchical clustering analysis (Ward method) in HCCs with and without Wnt/β-catenin activating mutations and classified these into an inflamed and a non-inflamed class based on the mRNA expressions associated with CD8+ T cells as shown in online supplementary Table 1, respectively. For the comparison of categorical variables, Pearson's χ^2 test or Fisher's exact test was applied. One-way analysis of variance or the Wilcoxon rank-sum test was used for comparison of continuous variables. The Kaplan-Meier survival

curves (log-rank test) were applied for comparison of OS and RFS. A two-tailed p value <0.05 was considered to indicate a statistically significant difference in all analyses. We refer to the Cancer Genome Atlas (TCGA) database for external validation (Liver HCC in TCGA (TCGA, Firehouse Legacy) annotated mutation and RNA expression data file from cBioPortal for Cancer Genomics (https://www.cbioportal.org/) on January 6, 2023, for 379 cases.

Statistical analyses were performed using the IBM Statistical Package for the Social Sciences Statistics version 28.0 (IBM, Armonk, NY, USA). Heat maps were described using internet software R v4.3.0 (https://cran.r-project.org/bin/windows/base/) and Morpheus (https://software.broadinstitute.org/morpheus/) by selecting only genes with F values >10 and p values <0.001.

Results

Patient Characteristics

Genetic analysis of 152 HCC tissues revealed 5 *APC* mutations, 35 *CTNNB1* mutations; no mutations were detected in the *AXIN1* and *AXIN2* genes in this cohort. Among the 35 CTNNB1 mutations, 21 cases had mutations in the D32-S37, 6 cases had mutations at T41 region of exon 3. Additionally, there were 6 cases with mutations at S45, 1 case with a mutation at N387, and 1 case with a mutation at T951 (supplementary dataset) [34]. Consequently, 40 HCCs (26.3%) carried mutations in Wnt/β-catenin pathway.

The median follow-up period was 107.3 months (95% CI: 93.5–121.2). Differences in baseline characteristics between HCCs without Wnt/β-catenin mutation (n = 112) and those with Wnt/β-catenin mutation (n = 40) are summarized in Table 1. For HCCs with Wnt/β-catenin mutations, the median patient age was 72.0 years (range 56–80), 85.5% were male (34/40), 3 patients were hepatitis B surface antigen positive, 18 patients were hepatitis C virus antibody positive, 7 patients were diagnosed with nonalcoholic steatohepatitis (NASH), 4 patients were heavy alcohol drinkers, and 8 patients had cryptogenic HCC. There were no significant differences in the clinical characteristics between the two groups except for a higher proportion of male patients in the group of HCC with Wnt/β-catenin activating mutations (p = 0.047).

Based on the comparison of characteristic for tumor status, HCC with Wnt/β-catenin mutation had a significantly larger tumor diameter (p = 0.024) and significantly lesser poorly differentiated forms (p = 0.021). CD8 T-cell infiltration was more prominent in tumors without Wnt/β-catenin mutation than those with the mutations, although this was not significant (p = 0.724). Comparing the expression of immune checkpoint molecules on TIL, there were no significant differences of expression in PD-1 (p = 0.767), CPS of PD-L1 (p = 0.221), and TIM-3 (p = 0.081) between the two groups. However, expression of LAG-3 was significantly less common in Wnt/β-catenin-mutated HCCs (Table 1). There were significant differences in gene expression between the two groups; increased expression of genes involved in the canonical β-catenin pathway and hepatocyte differentiation, such as *AXIN2*, *GLUL*, and *SLCO1B3* in HCCs with Wnt/β-catenin activating mutations. Conversely, gene expression of biliary stem cell markers (*EpCAM*, *SALL4*, and *KRT19*), EMT-related genes (*SNAI1, SNAI3*, and *TWIST*), transcription factor *FOXM1* that defines aggressive tumor traits, and other signaling pathways such as *TGF-B1, FGF19, VEGFB, CCL4*, and *CCL5*, was significantly increased in HCCs without Wnt/β-catenin mutations (Table 1).

The RFS of the two groups after curative tumor resection is shown in online supplementary Figure 1a. HCCs with Wnt/β-catenin mutation had a better RFS (median RFS 28.9 vs. 15.9 months, p = 0.181, hazard ratio 0.683) with a 1-year recurrence rate of 22.5% (vs. 42.9%) and a 2-year recurrence rate of 37.5% (vs. 60.7%) in spite of the larger baseline tumor diameter. The median OS of patients with HCCs with Wnt/β-catenin mutation was 117.2 months (95% CI 92.9–141.5) and tended to be longer than that of HCCs without Wnt/β-catenin mutation (57.9 months, 95% CI 56.5–95.3) although this difference was not significant (online suppl. Fig. 1b).

Immune Class in HCCs with and without Wnt/β-Catenin Mutation

Referring to the data of immune-related molecules published by Sia et al. [33], we performed a principal component analysis by gene expression levels of CD8+ T cells and IFN-γ signaling (shown in online suppl. Table 1) in 136 cases with RNA of suitable quality for sequence among a total of 152 HCCs. A heat map based on significant mRNA expression levels of these immune-related molecules showed heterogeneity of the immunological TME in HCC with Wnt/β-catenin mutation (Fig. 1a). Most HCCs with Wnt/β-catenin mutation were characterized as non-inflamed and immune-cold TMEs that expressed few inflamed markers related to TIL, TGF-β1, and IFN-γ signal. In contrast, a small number of HCCs with Wnt/β-catenin mutation showed high expression of genes suggestive of CD8+ cell infiltration and activation of IFN-γ/TGF-β1 signaling (Fig. 1a).

Hierarchical clustering analysis was performed using expression of genes involved in CD8+ T cell infiltration in 136 cases with RNA of suitable quality for sequence among a total of 152 HCCs, and classified into inflamed class (n = 25) and non-inflamed class (n = 111). Comparison of RFS by inflamed or non-inflamed classes showed a trend toward better RFS in the inflamed class

Table 1. Patient characteristics based on the presence or absence of *Wnt/β-catenin* mutation

	Absence for *Wnt/β-catenin* mutation (n = 112)	Presence for *Wnt/β-catenin* mutation (n = 40)	p value
Clinical background			
Age, median (range), years	68.0 (35–85)	72.0 (56–80)	0.167
Sex, male	68.8% (77/112)	85.5% (34/40)	0.047
Etiology, HBV/HCV/NASH/alcohol/others	27/46/11/4/25	3/18/7/4/8	0.131
F stage, 0/1/2/3/4	1/6/10/26/66	0/4/5/11/20	0.682
WBC, median (IQR), 10^3/μL	5.90 (4.2–8.0)	5.90 (4.6–8.2)	0.796
NLR, median (IQR)	2.05 (1.47–3.69)	1.77 (1.2–2.9)	0.128
Platelets, median (IQR), 10^3/μL	15.9 (12.3–19.7)	19.3 (14.0–23.3)	0.203
RDW, median (IQR)	12.4 (11.8–13.2)	12.5 (11.7–13.3)	0.458
CRP, median (IQR), mg/dL	0.208 (0.068–1.989)	0.249 (0.075–1.05)	0.886
Hyaluronic acid, median (IQR), ng/mL	132.1 (72.2–282.9)	142.1 (59.0–240.8)	0.837
Serum albumin, median (IQR), g/dL	3.8 (3.3–4.1)	3.8 (3.5–4.2)	0.617
Total bilirubin, median (IQR), mg/dL	0.75 (0.50–1.10)	0.70 (0.53–0.98)	0.346
ALT, median (IQR), U/L	42 (24.0–84.0)	57 (32.3–103.3)	0.767
LDH, median (IQR), U/L	225 (185–296)	221 (203–258)	0.449
Corrected calcium, median (IQR), mg/dL	9.4 (9.2–9.7)	9.5 (9.2–9.7)	0.901
Tumor status			
Tumor size, median (range), cm	3.5 (1.0–15.0)	4.5 (1.6–15.0)	0.024
Microvascular invasion, yes	29.5% (33/112)	25.0% (10/40)	0.584
HCC differentiation, well/moderate/poor	7/76/28	0/37/3	0.021
AFP level, median (IQR), ng/mL	24.0 (5.50–143.0)	5.50 (4.00–25.8)	0.913
DCP, median (IQR), mAU/mL	59.0 (24.0–707.0)	143.5 (37.5–638.2)	0.246
Immunological TME, IHC			
PD-L1, positive	37.7% (31/112)	17.5% (7/40)	0.221
PD-1, positive	19.6% (22/112)	17.5% (7/40)	0.767
LAG-3, positive	25.5% (28/112)	10.0% (4/40)	0.046
TIM-3, positive	25.9% (29/112)	12.5% (5/40)	0.081
Gene expression related to Wnt/β-catenin, immune signaling-related pathways[1]			
AXIN2, median (IQR)	1.8 (0.77–3.7)	22.5 (3.7–38.4)	<0.001
GLUL, median (IQR)	319 (226–523)	1,577 (592–4,969)	<0.001
EpCAM, median (IQR)	5.5 (0.73–55.1)	0.52 (0.20–2.3)	<0.001
SALL4, median (IQR)	2.9 (1.08–7.9)	0.34 (0.65–2.55)	0.017
KRT19, median (IQR)	0.97 (0.08–5.4)	0.10 (0.0–1.4)	0.044
SNAI1, median (IQR)	3.0 (1.4–6.1)	1.4 (0.63–2.8)	0.002
SNAI3, median (IQR)	0.17 (0.07–0.36)	0.0 (0.0–0.08)	<0.001
TWIST1, median (IQR)	0.30 (0.08–0.67)	0.13 (0.06–0.38)	0.017
TGFB1, median (IQR)	25.1 (15.2–58.4)	12.7 (7.5–22.6)	<0.001
IFNG, median (IQR)	0.40 (0.15–1.03)	0.19 (0.07–0.52)	0.250
FGF19, median (IQR)	1.22 (0.22–14.2)	0.07 (0.0–0.70)	<0.001
VEGFB, median (IQR)	28.8 (12.5–47.8)	7.2 (3.4–16.4)	<0.001
CCL4, median (IQR)	16.7 (7.8–31.7)	7.8 (3.2–17.9)	0.017
CCL5, median (IQR)	19.6 (9.8–41.0)	12.6 (4.6–23.1)	0.017
HNF4A, median (IQR)	108.3 (73.5–166.2)	111.3 (81.6–148.2)	0.583
FOXM1, median (IQR)	11.2 (4.4–21.5)	5.4 (2.5–13.6)	0.036
SLCO1B3, median (IQR)	2.23 (0.35–13.7)	32.8 (2.0–104.0)	<0.001
Outcome			
1-year recurrence rate	42.9% (48/112)	22.5% (9/40)	0.020
2-year recurrence rate	60.7% (68/112)	37.5% (15/40)	0.010
Extrahepatic recurrence rate	8.0% (9/112)	7.5% (3/40)	0.903

HCV, hepatitis C virus; HBV, hepatitis B virus; NBNC, negative for hepatitis B surface antigen and hepatitis C antibody; NASH, nonalcoholic steatohepatitis; WBC, white blood cell; NLR, neutrophil-lymphocyte ratio; RDW, red blood cell distribution width; CRP, C-reactive protein; AST, aspartate aminotransferase; ALT, alanine aminotransferase; LDH, lactate dehydrogenase; AFP, α-fetoprotein; DCP, des-γ-carboxy prothrombin; IQR, interquartile range; PD-1, programmed cell death protein 1; PD-L1, programmed death-ligand 1; TIM-3, T-cell immunoglobulin mucin-3; LAG-3, lymphocyte-activation gene-3; GLUL, glutamate-ammonia ligase; EpCAM, anti-epithelial cell adhesion molecule; SALL4, Spalt-like4; KRT19, cytokeratin 19; VEGF, vascular endothelial growth factor; FGFR, fibroblast growth factor receptors; MMP, matrix metalloproteinase; TGFB, transforming growth factor-β; IFNG, interferon gamma; CCL, CC chemokine ligand; CXCL, chemokine (C-X-C motif) ligand; HNF, hepatocyte nuclear factor; FOX, forkhead box; SLCO1B3, solute carrier organic anion transporter 1B3. [1]Expressions of mRNA were determined through the mRNA sequencing.

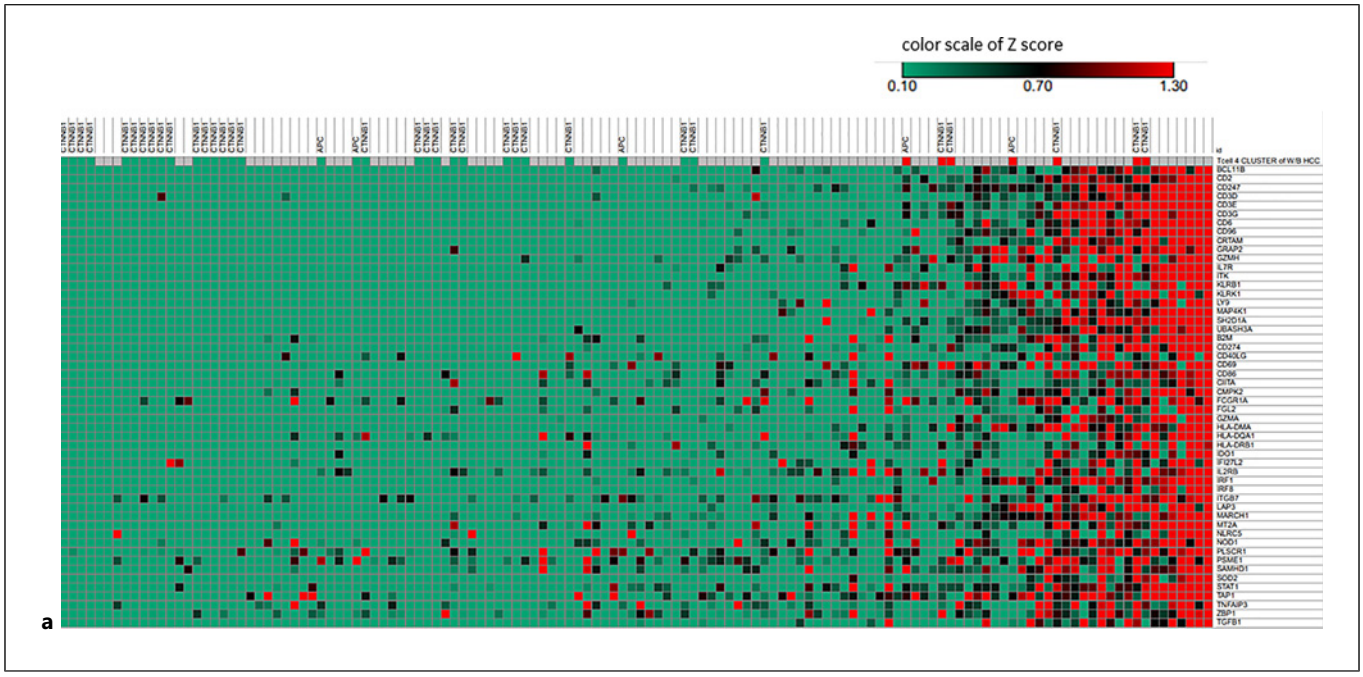

1

(Figure continued on next page.)

(online suppl. Fig. 1c), with little difference in OS (online suppl. Fig. 1d). Additionally, among the 136 HCCs evaluated by IHC, in the inflamed class of 25 HCCs, 16 HCCs exhibited T cells with exhausted phenotypes expressing PD-1, LAG-3, or TIM-3. When comparing the expression levels of the 9-gene signature (*LAG3, CD244, CCL5, CXCL9, CXCL13, MSR1, CSF3R, CYBB, and KLRK1*) as presented by Hsu et al. [35], all nine factors were significantly upregulated in the inflamed class HCCs (n = 25) compared to the non-inflamed class HCCs (n = 111) (online suppl. Fig. 2, $p < 0.001$).

Next, we further focused on the 40 HCCs with Wnt/β-catenin mutation; HCCs with Wnt/β-catenin mutation were classified into inflamed and non-inflamed classes (Fig. 1b). The non-inflamed class (n = 33, 82.5%) and inflamed class (n = 7, 17.5%) of HCCs with Wnt/β-catenin mutation were marked in the top panel of Figure 1a in green and red, respectively. IHC also confirmed that intratumor T-cell infiltration stained with CD3, CD4, and CD8 was significantly more pronounced in the inflamed class. CD3+ cell (7.49 cells/HPF vs. 91.2 cells/HPF, $p < 0.001$), CD4 (2.43 cells/HPF vs. 35.1 cells/HPF, $p = 0.013$), CD8 (5.93 cells/HPF vs. 72.9 cells/HPF, $p < 0.001$) in non-inflamed and inflamed classes, respectively (Fig. 1c). Furthermore, among 7 inflamed class HCCs with Wnt/β-catenin mutations, 4 HCCs were classified into the T-cell exhausted phenotype positive for PD-1, LAG-3, or TIM-3, while 3 HCCs were classified into the non-exhausted inflamed class. The comparison with patient baseline characteristics of two distinct classes with and without Wnt/β-catenin mutation is shown in Table 2. There were significant differences in the etiologies of the two classes with hepatitis B/C virus-related HCC accounting for 54.5% (18/33) of the non-inflamed class and alcohol-induced HCC accounting for 42.9% (3/7) of the inflamed class of HCC with Wnt/β-catenin mutation; however, there were no significant differences in other factors between the two classes of HCC with Wnt/β-catenin mutation. Regarding tumor differentiation, poorly differentiated HCC was more frequently observed in the inflamed class than in the non-inflamed class (p = 0.047).

The RFS for each immune class of HCC with and without Wnt/β-catenin mutation is shown in Figure 2; online supplementary Figure 1e. In HCC without Wnt/β-catenin mutations, RFS did not differ depending on whether the patient belonged to the inflamed or non-inflamed class (online suppl. Fig. 1e). On the other hand, in HCCs with Wnt/β-catenin mutations, there was a significant difference between the two distinct classes; the median RFS was not achieved in HCC cases with Wnt/β-catenin mutation in the inflamed class. Conversely, the HCCs cases with Wnt/β-catenin mutation in the non-inflamed class showed a median RFS of

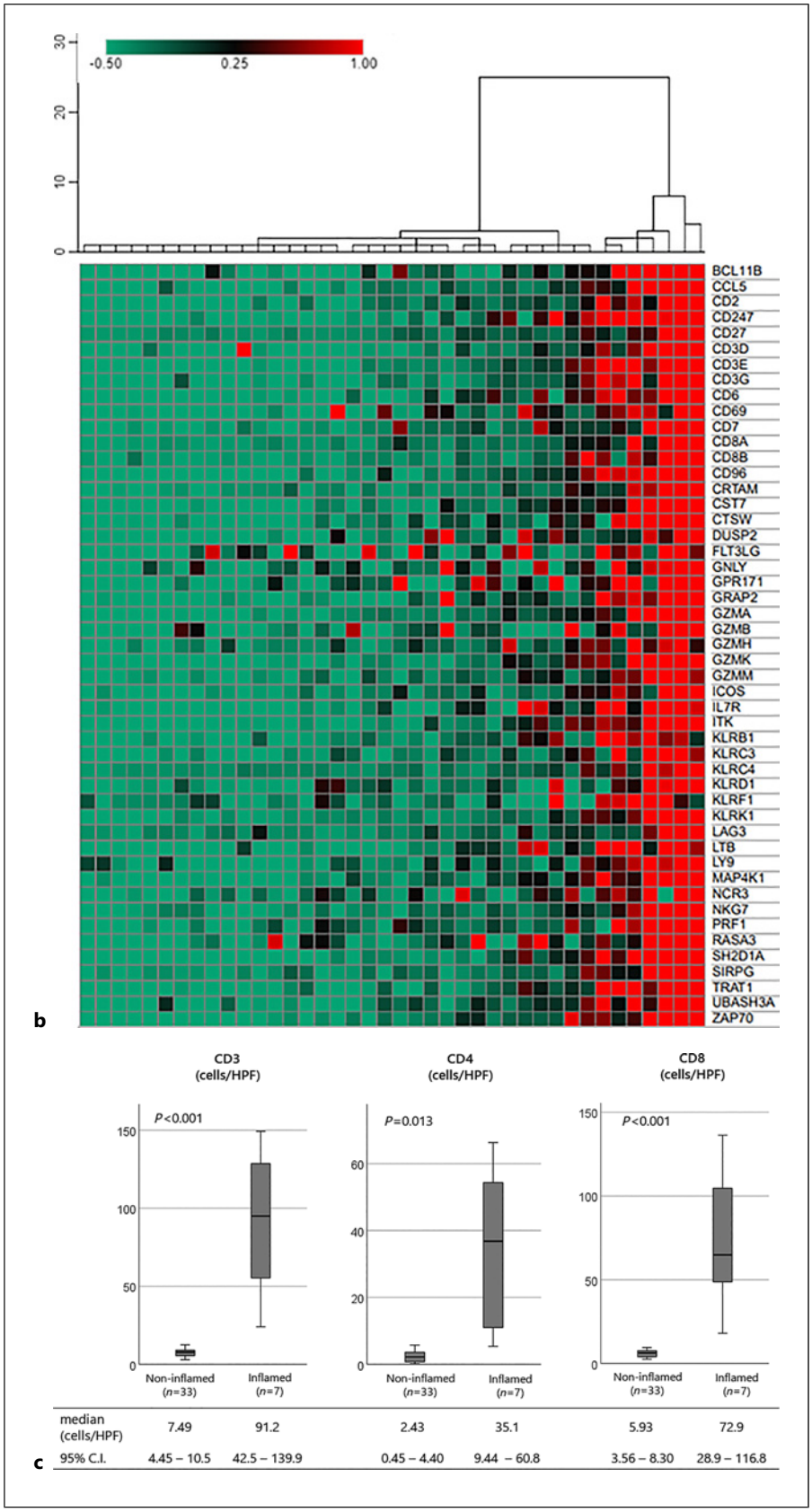

Fig. 1. a Heatmap based on principal component analysis using the genes associated with CD8+ T cell activation. Principal component analysis was performed on gene expression for TIL activation across 152 HCCs, and a heat map was generated based on the results; cases with gene mutations such as *CTNNB1* and *APC* were labeled. **b** Hierarchical cluster analysis using the genes associated with CD8+ T-cell activation. Based on the gene expression levels associated with CD8+ T cells obtained from the transcriptome analysis (see online suppl. Table 1) in 40 HCC cases with Wnt/β-catenin mutations, a cluster analysis was performed and generated a heat map with *Z* values. The patients were classified into two groups: those with high gene expression (inflamed class, 7 cases) and those with low gene expression (non-inflamed class, 33 cases). **c** Immunostaining for lymphocytes infiltrating in the tumor. Non-inflamed and inflamed classes of Wnt/β-Catenin mutated HCCs, which classified according to RNA expression levels associated with CD8+ T cells, were performed to evaluate lymphocyte infiltration into tumor. The cells stained by CD3, CD4, and CD8 were counted as cells/HPF. The inflamed class HCC showed significantly more T-cell infiltration. HCC, hepatocellular carcinoma.

20.8 months (95% CI: 0.00–43.1) and a significantly higher risk of postoperative recurrences (hazard ratio 0.200, 95% CI: 0.046–0.867, $p = 0.018$) (Fig. 2). A similar trend was observed in OS, and the results of the survival analysis for each immune class are shown in online supplementary Figure 1f, g.

We performed external validation using the same hierarchical clustering analysis with HCC cohort with Wnt/β-catenin mutation from the TCGA database ($n = 129$) (online suppl. Fig. 3a), indicating that HCCs with Wnt/β-catenin mutation showed two major immune classes: non-inflamed and inflamed types. The RFS and OS for each immune class of HCC with Wnt/β-catenin mutation are shown in online supplementary Figure 3b. The median RFS was 36.7 (95% CI: 12.7–60.7) in inflamed class of HCCs with Wnt/β-catenin mutation and was 19.4 (95% CI: 13.5–25.4) in non-inflamed class of HCCs ($p = 0.074$). The median OS was not reached in inflamed class of HCCs with Wnt/β-catenin mutation and was 33.0 (95% CI: 9.04–57.0) in non-inflamed class ($p = 0.014$).

The transcriptome analysis revealed different patterns in the expression of genes involved in the Wnt/β-catenin pathway, tumor differentiation, EMT, and chemokine: *AXIN2* (median values: 24.0 vs. 5.1 for non-inflamed vs. inflamed class, $p = 0.032$), *CTNNB1* (486.2 vs. 370.0, $p = 0.080$), *CLUL* (3,179.8 vs. 664.2, $p = 0.028$), *SNAI3* (0.0 vs. 0.23, $p = 0.005$), *VIM* (200.1 vs. 359.4, $p = 0.009$), *TGFB1* (11.1 vs. 23.8, $p = 0.007$), *IFN-γ* (0.14 vs. 2.28, $p < 0.001$), *MMP9* (1.30 vs. 14.7. $p = 0.054$), *NOTCH3* (8.99 vs. 11.0, $p = 0.020$), *CCL4* (5.42 vs. 26.9, $p = 0.032$), *CCL5* (11.2 vs. 84.8, $p < 0.001$), *CXCL10* (32.9 vs. 259.5, $p = 0.006$), *CXCL11* (3.14 vs. 26.0, $p < 0.001$) in HCCs with Wnt/β-catenin mutation (Table 2; Fig. 3a). In the inflamed class of HCCs without Wnt/β-catenin mutations, *TGFB1, SNAI3, VIM, MMP9, VEGFB, CCL4, and CCL5* were the most upregulated in the four groups and *HNF4A* was most downregulated in the four groups (shown in Table 2; Fig. 3a). Focusing on HNF4A, its expression decreases in the inflamed class of HCCs without Wnt/β-catenin mutation, whereas in HCCs with Wnt/β-catenin mutation, no significant difference in expression levels was observed between the inflamed and non-inflamed classes. The comparison of the frequencies of oncogenic mutations between the two groups is shown in Table 3. The gene mutations were classified based on the oncogenic pathway involved; none of which showed significant differences in the two immune classes.

Comparison of expressions of molecules related to TME and tumor differentiation based on IHC showed the following (Table 2; Fig. 1c): intratumor T-cell infiltration stained with CD8 was more prominent in the inflamed class of HCCs with Wnt/β-catenin mutation (5.93 cells/HPF vs. 72.9 cells/HPF for non-inflamed vs. inflamed class, $p < 0.001$) and correlated strongly with mRNA expression levels. The mRNA expression of *AXIN2* and *CTNNB1*, was significantly higher in the non-inflamed class of HCC with Wnt/β-catenin mutation, while there was no difference in nuclear deposition of β-catenin between the two classes (63.6% vs. 42.9%, $p = 0.528$). mRNA expression of *GLUL* and the intensity of GS expression in IHC, both known markers of hepatocyte differentiation, were significantly higher in the non-inflamed class of HCCs compared to the inflamed class (3,179.8 vs. 664.2, $p = 0.028$ for *GLUL* mRNA, and 60.0% vs. 14.3%, $p = 0.047$ for GS staining, respectively). Transcriptome analysis showed no significant difference in gene expression of biliary stem cell markers or *FOXM1* between the two classes, while EpCAM-positive (0% vs. 14.3%, $p = 0.028$) or FOXM1-positive (9.1% vs. 42.9, $p = 0.011$) HCC cells were significantly more abundant in the inflamed class. The representative figures of FOXM1 IHC in this study are shown in online supplementary Figure 4. Typical cases with Wnt/β-catenin mutated HCC classified into non-inflamed and inflamed class are shown in Figure 4b–t.

The discriminatory ability to separate into inflamed and non-inflamed classes was compared by ROC analysis (results for all HCCs are shown in online suppl. Fig. 5a, results for the 40 HCCs with Wnt/β-catenin mutations are shown in online suppl. Fig. 5b, and result of external validation with TCGA dataset are shown in online suppl. Fig. 5c). When examining RNA expression levels, most of the markers associated with CD8+ T cells used in this cluster analysis were found to have high discriminatory power with an AUROC of 0.90 or higher ($p < 0.001$), and HNF4A and FOXM1/HNF4A ratio may be useful to separate two classes (shown in online suppl. Fig. 5a–c). Clinical parameters showed that the alpha-fetoprotein/des-γ-carboxyprothrombin ratio significantly differentiated the inflamed and non-inflamed classes ($p = 0.021$), but not in the 40 HCCs with Wnt/β-catenin mutations (shown in online suppl. Fig. 5a, b).

The Heterogeneity of MRI Images in Wnt/β-Catenin Mutated HCC

As enhancement of Gd-EOB-DTPA on MRI was known to be attributed to the expression of OATP1B3, which was a downstream target of Wnt/β-catenin signal, we examined the images of Gd-EOB-DTPA-enhanced MRI for HCC with Wnt/β-catenin mutation. Sixteen of 40 patients with Wnt/β-catenin mutated HCCs underwent Gd-EOB-DTPA-enhanced MRI examination within 1 month before surgery; comparison of the hepatobiliary phase revealed that all intrahepatic nodules in the inflamed class had lower signal intensity than

Table 2. Characteristic according to immune class in HCCs with and without Wnt/β-catenin mutation

	HCCs with Wnt/β-catenin mutation			HCCs without Wnt/β-catenin mutation		
	non-inflamed class (*n* = 33)	inflamed class (*n* = 7)	*p* value	non-inflamed class (*n* = 78)	inflamed class (*n* = 18)	*p* value
Clinical background						
Age, median (range), years	72 (58, 80)	72 (56, 80)	0.865	67 (45, 84)	72 (57, 79)	0.109
Sex, male	84.8% (28/33)	85.7% (6/7)	0.954	69.2% (54/78)	66.7% (12/18)	0.787
Etiology, HBV/HCV/NASH/AL/Other	3/15/8/1/6	0/3/1/3/0	0.021	23/26/10/4/15	2/12/0/0/4	0.054
NLR, median (IQR)	1.78 (1.29, 2.99)	1.76 (0.86, 2.94)	0.370	2.22 (1.54, 3.81)	1.98 (1.40, 2.95)	0.794
PLT, median (IQR) (10^3/μL)	19.4 (14.0, 23.7)	17.6 (9.1, 21.4)	0.751	14.6 (9.9, 21.6)	14.6 (11.6, 20.5)	0.794
CRP, median (IQR), mg/dL	0.258 (0.77, 0.91)	0.196 (0.07, 3.23)	0.574	0.281 (0.60, 2.44)	0.143 (0.10, 0.33)	0.067
Serum albumin, median (IQR), g/dL	3.8 (3.4, 4.1)	3.6 (3.5, 4.4)	0.499	3.8 (3.3, 4.1)	3.9 (3.1, 4.2)	0.512
Total bilirubin, median (IQR), mg/dL	0.80 (0.60, 1.1)	0.50 (0.40, 0.80)	0.103	0.80 (0.50, 1.2)	0.70 (0.50, 1.08)	0.335
ALT, median (IQR), U/L	57 (36, 128)	55 (30, 101)	0.321	43 (26, 84)	30 (17, 73)	0.433
AFP, median (IQR), ng/mL	5.0 (3.0, 24.0)	4.0 (2.0, 2,044)	0.796	40.5 (6.75, 450)	86.5 (18.0, 501.5)	0.794
DCP, median (IQR), mAU/mL	177.0 (46.5, 845)	133 (42, 1,414)	0.494	215 (31.0, 1,849)	79 (23, 190)	0.306
Tumor status/IHC						
Tumor size, median (range) (cm)	5.0 (2.0, 15)	3.1 (1.6, 7.6)	0.141	4.9 (1.0, 15)	3.0 (1.0, 12.0)	0.067
Microvascular invasion, yes	21.2% (7/33)	42.9% (3/7)	0.310	33.3% (26/78)	27.8% (5/18)	0.650
HCC differentiation, well/moderate/poor	0/30/3	0/5/11, NE due to necrosis	0.047	3/57/18	2/11/5	0.365
CD8+ T cell, median (IQR)	0.495% (0.09, 1.99)	8.12% (1.2, 20.8)	0.001	1.40% (0.12, 6.69)	3.04% (0.76, 14.6)	0.021
Nuclear localization of β-catenin, positive	63.6% (21/33)	42.9% (3/7)	0.528	ND	ND	NE
GS, positive	60.0% (20/33)	14.3% (1/7)	0.047	ND	ND	NE
FOXM1, positive	9.1% (3/33)	42.9% (3/7)	0.011	ND	ND	NE
CK19, positive	9.1% (3/33)	14.3% (1/7)	0.574	ND	ND	NE
SALL4, positive	0.0% (0/33)	0.0% (0/7)	NE	ND	ND	NE
EpCAM, positive	0.0% (0/33)	14.3% (1/7)	0.028	ND	ND	NE
PD-L1, positive	9.1% (3/33)	57.1% (4/7)	0.002	24.4% (19/78)	38.9% (7/18)	0.448
PD-1, positive	9.1% (3/33)	57.1% (4/7)	0.002	14.1% (11/78)	33.3% (6/18)	0.002
LAG-3, positive	3.0% (1/33)	42.9% (3/7)	0.001	14.4% (11/78)	55.6% (10/18)	<0.001
TIM-3, positive	6.1% (2/33)	42.9% (3/7)	0.008	20.5% (16/78)	44.4% (8/18)	0.002

Liver Cancer 2024;13:285–305
DOI: 10.1159/000533818

Table 2 (continued)

	HCCs with Wnt/β-catenin mutation			HCCs without Wnt/β-catenin mutation		
	non-inflamed class (*n* = 33)	inflamed class (*n* = 7)	*p* value	non-inflamed class (*n* = 78)	inflamed class (*n* = 18)	*p* value
Gene expression by transcriptome analysis						
AXIN2, median (IQR)	24.0 (4.9–44.2)	5.1 (2.6–11.4)	0.032	1.65 (0.74–3.70)	2.04 (1.15–3.72)	0.794
CTNNB1, median (IQR)	486.2 (349.7–777.9)	370.0(330.7–408.0)	0.080	381.0 (308.9–496.4)	385.0 (329.5–470.3)	0.794
GLUL, median (IQR)	3,179.8 (836.7–5,351.5)	664.2 (178.8–1,331.4)	0.028	319.5 (225.1–541.2)	303.9 (225.6–468.5)	0.794
HNF1A, median (IQR)	28.5 (24.9–37.6)	21.9 (21.1–24.7)	0.018	28.9 (20.4–39.5)	22.1 (12.3–32.2)	0.067
HNF4A, median (IQR)	112.2 (83.2–147.9)	93.5 (53.3–151.9)	0.328	120.0 (85.9–185.4)	65.9 (27.1–118.7)	0.001
FOXM1, median (IQR)	5.23 (2.66–14.0)	7.37 (1.31–13.5)	0.589	11.5 (4.66–21.0)	7.79 (2.37–39.2)	0.266
SNAI3, median (IQR)	0.0 (0.0–0.07)	0.23 (0.06–0.39)	0.005	0.14 (0.61–0.29)	0.44 (0.21–0.96)	0.004
VIM, median (IQR)	200.1 (141.8–328.6)	359.4 (328.5–478.3)	0.009	265.8 (178.1–433.7)	671.7 (351.7–2,231.1)	0.004
TGFB1, median (IQR)	11.1 (6.3–18.6)	23.8 (17.7–29.3)	0.007	19.5 (13.0–47.1)	62.7 (34.3–92.2)	<0.001
IFNG, median (IQR)	0.14 (0.06–0.30)	2.28 (0.77–2.98)	<0.001	0.29 (0.13–0.60)	2.06 (0.86–5.64)	<0.001
MMP9, median (IQR)	1.30 (0.80–2.95)	14.7 (5.57–31.7)	0.054	5.55 (1.83–15.4)	31.1 (7.35–59.3)	0.019
NOTCH3, median (IQR)	8.99 (6.2–11.4)	11.0 (7.1–26.2)	0.020	11.0 (5.97–18.9)	18.0 (7.9–28.8)	0.433
TP53, median (IQR)	18.0 (13.2–33.1)	26.8 (19.6–57.9)	0.077	30.6 (17.7–55.6)	40.6 (28.0–60.8)	0.433
CCL4, median (IQR)	5.42 (2.9–13.4)	26.9 (10.3–49.1)	0.032	12.7 (7.0–22.7)	55.2 (24.4–64.9)	0.004
CCL5, median (IQR)	11.2 (4.1–14.8)	84.8 (36.1–113.2)	<0.001	16.4 (8.2–32.9)	102.3 (52.1–155.4)	<0.001
CXCL10, median (IQR)	32.9 (12.3–76.5)	259.5 (20.1–462.1)	0.006	36.7 (15.8–70.6)	131.7 (57.0–257.4)	0.019
CXCL11, median (IQR)	3.14 (0.8–6.7)	26.0 (3.0–83.9)	<0.001	3.26 (0.98–6.97)	14.1 (4.3–25.3)	0.004
VEGFB, median (IQR)	6.00 (3.2–11.9)	16.4 (8.2–20.3)	0.037	27.0 (12.2–48.0)	34.4 (19.0–46.7)	0.794

HCC, hepatocellular carcinoma; EMT, epithelial to mesenchymal transition; CTNNB1, catenin beta-1; HCV, hepatitis C virus; HBV, hepatitis B virus; NBNC, negative for hepatitis B surface antigen and hepatitis C antibody; NASH, nonalcoholic steatohepatitis; NLR, neutrophil-lymphocyte ratio; RDW, red blood cell distribution width; CRP, C-reactive protein; ALT, alanine aminotransferase; AFP, α-fetoprotein; DCP, des-γ-carboxy prothrombin; IQR, interquartile range; PD-1, programmed cell death protein 1; PD-L1, programmed death-ligand 1; TIM-3, T-cell immunoglobulin mucin-3; LAG-3, lymphocyte-activation gene-3; GLUL, glutamate-ammonia ligase; EpCAM, anti-epithelial cell adhesion molecule; SALL4, Spalt-like4; KRT19, cytokeratin 19; VEGF, vascular endothelial growth factor; FGFR, fibroblast growth factor receptors; MMP, matrix metalloproteinase; TGFB, transforming growth factor-β; IFNG, interferon gamma; CCL, CC chemokine ligand; CXCL, chemokine (C-X-C motif) ligand; NE, not evaluated; ND, no data.

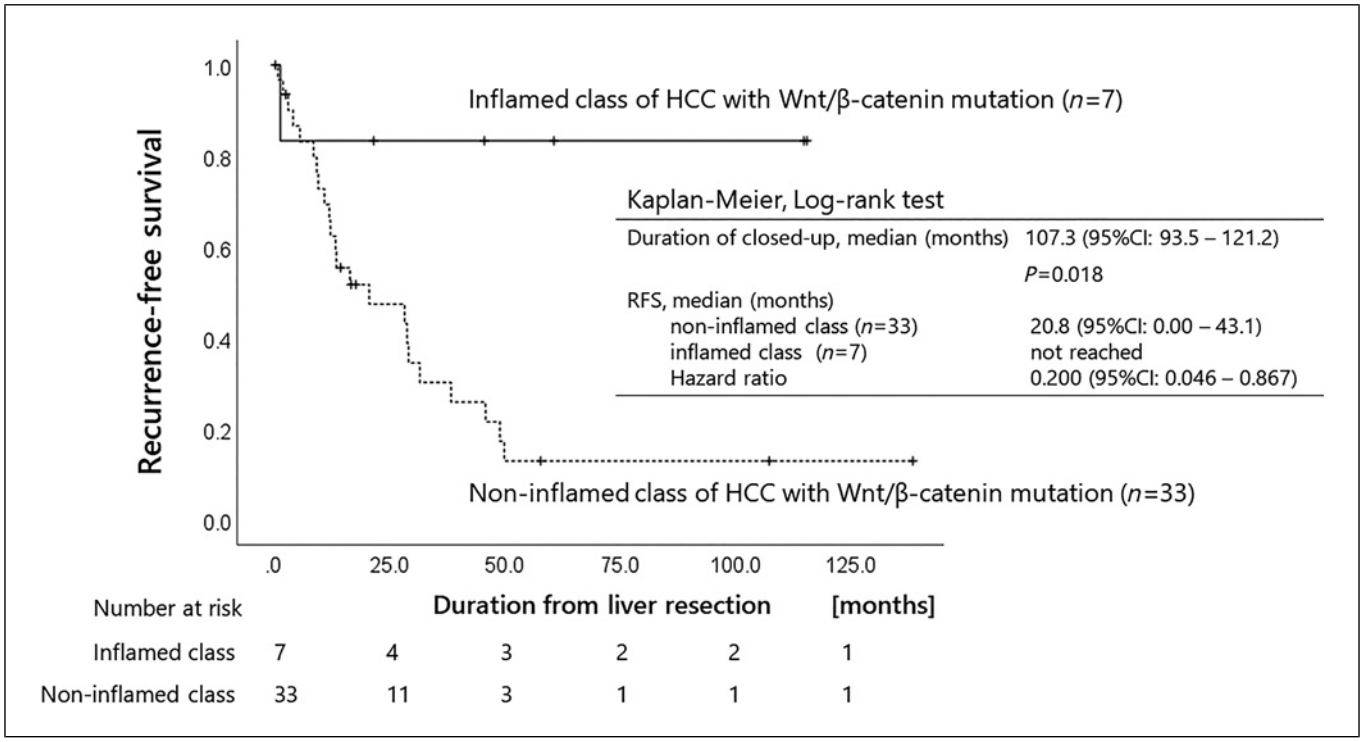

Fig. 2. Recurrence-free survival by immune class among HCCs with Wnt/β-catenin mutations. Postoperative recurrence rates were compared in 40 HCCs with Wnt/β-catenin mutations. The median RFS for the inflamed class (N = 7) was not achieved, while the median RFS for the non-inflamed class (N = 33) was 20.8 months (95% CI: 0.00–43.1). The postoperative recurrence rate was significantly lower in the inflamed class (Kaplan-Meier, Log-rank test, p = 0.018). HCC, hepatocellular carcinoma; RFS, recurrence-free survival; CI, confidence interval.

the background liver. In contrast, compared to the background liver, the intrahepatic nodules in the non-inflamed class showed iso to higher signal intensity on EOB-MRI; the mean RER was 0.99 (95% CI: 0.85–1.15) for the non-inflamed class of HCCs (n = 13) and 0.66 (95% CI: 0.38–0.93) for the inflamed class of HCCs (p = 0.065, results shown in Fig. 4a). The representatives of hematoxylin and eosin staining and IHC of HCC cells, and the hepatobiliary phase on Gd-EOB-DTPA-enhanced MRI are presented in Figure 4b.

Comparison of the TME in Two Immune Phenotypes of HCCs with Wnt/β-Catenin Mutation

Next, we compared the TME in the two phenotypes of HCCs with Wnt/β-catenin mutation. For the classification of TME based on each immune step and their involved gene expressions, we refereed to the previous study, which was reported to better represent the immune status [26].

The seven molecular profiles of TME selected for this comparison were as follows: innate immunity, priming and activation, IFN-γ response, inhibitory molecules, Treg cells, MDSCs, and tumor cell recognition. Using genes associated with these seven gene ontologies [26–28] (shown in online suppl. Table 1), cluster analysis was performed using mRNA expression of the genes involved in the seven immune steps for 40 HCCs with Wnt/β-catenin mutations. For heat mapping, the data were normalized using the z-score for the entire 40 cases (shown in online suppl. Fig. 6). Of the selected molecular profiles, IFN-γ response was classified into three groups (highly activated, moderately activated, not activated), while the remaining six parameters were classified into two groups (activated, not activated), revealing the heterogeneity of the immunological TME in HCCs with Wnt/β-catenin mutations.

A small proportion (n = 7) of HCCs with Wnt/β-catenin mutations, classified as inflamed because of the enhanced expression of the genes involved in activation of CD8+ T cells, had high to moderate activation of IFN-γ signaling, consistent with a previous report [33]. In addition, other immune steps were revealed to be enhanced in this class, including innate immunity involving natural killer cells, antigen presentation and priming by DCs, inhibitory molecules involved in immune escape, and suppressor system cells (Treg, MDSC) were activated (Fig. 5).

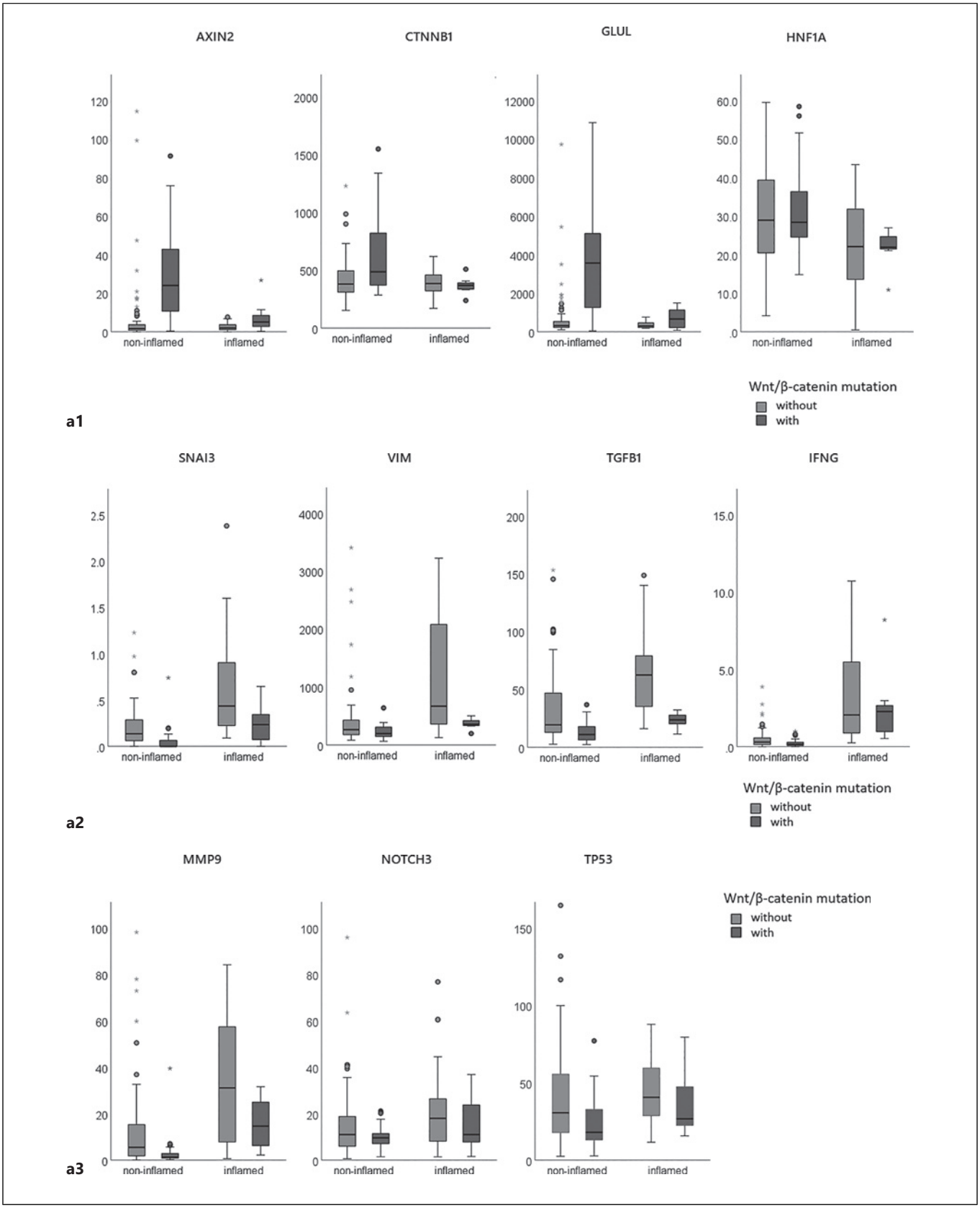

3

(Figure continued on next page.)

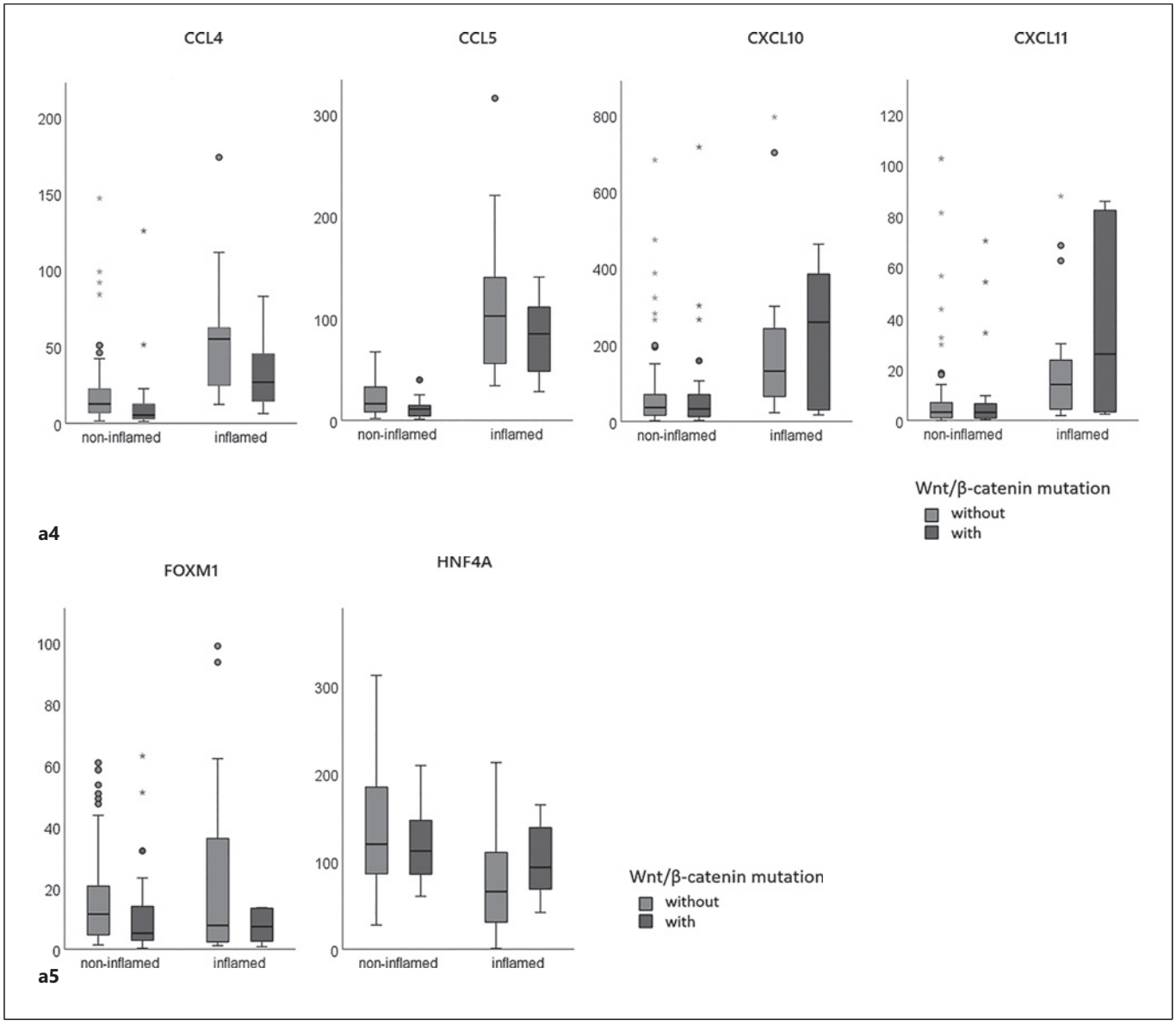

Fig. 3. a Gene expression levels between two immune classes of HCC with and without Wnt/β-catenin mutation. Gene expression levels obtained from transcriptome analysis were compared between the two immune classes. The non-inflamed class HCC with Wnt/β-catenin mutation (N = 33) had higher expression of *AXIN2* and *CTNNB1,* and *GLUL*. The inflamed class HCC with Wnt/β-catenin mutation (N = 7) had significantly lower expression of *GLUL* and higher expression of EMT-related genes such as *SNAIL3* and *VIM, TGFB1,* IFN-γ, *MMP9*, and *NOTCH3*. In addition, the expression levels of chemokines such as *CCL4* and *CCL5*, which are involved in dendritic cell migration, were significantly upregulated in the immune cold class. HCC, hepatocellular carcinoma; EMT, epithelial to mesenchymal transition; CTNNB1, catenin beta-1; GLUL, glutamate-ammonia ligase; TGFβ, transforming growth factor-β; IFN-γ, interferon gamma; MMP, matrix metalloproteinase; CCL, CC chemokine ligand; CXCL, chemokine (C-X-C motif) ligand.

Based on these data, HCCs with Wnt/β-catenin mutations were classified into two classes of TME according to molecular profile. Although IHC revealed similar ratios of cases with nuclear deposition of β-catenin in both classes, significant differences in the GS expression, which was the downstream target of Wnt/β-catenin signaling and cell differentiation marker, were observed (Fig. 5; Table 3).

Table 3. Number of genetic mutations by immune class

Altered pathway	Altered gene	Non-inflamed class (n = 33)	Inflamed class (n = 7)	p value (Fisher)
p53/cell cycle control pathway	*ATM, ATR, CCND1, CCND2, CCNE1, CDK12, CDKN2A, CREBBP, FBXW7, MDM2, RB1, RPS6KA2, TP53*	30.3% (10/33)	14.3% (1/7)	0.412
Chromatin remodeling	*ARID1A, ARID1B, ARID2, CREBBP, EZH2, SMARCA2,*	27.3% (9/33)	14.3% (1/7)	0.653
PI3K-Akt pathway	*PI3KCA, PI3KC2B, PI3KCB, PTEN, MAP3K7, RPS6CA2, TSC1, TSC2*	9.1% (3/33)	14.3% (1/7)	1.000
Oxidative and endoplasmic reticulum stress	*ATF1, CYP2C19, KEAP1, NFE2L2, ROS1*	18.2% (6/33)	14.3% (1/7)	1.000
DNA repair	*ATM, ERCC2, ERCC5, FANCA, MLH1, MSH2, MSH6, XZCC2*	6.1% (2/33)	0% (0/7)	1.000
Epigenetic regulator	*DNMT3A, IDH1, IDH2, KMT2A, KMT2B, KMT2C, KMT2D, SETD2, TET1, TET2*	21.2% (7/33)	28.6% (2/7)	1.000

Discussion

In our cohort, 136 HCCs subjected to RNA sequence, 25 HCCs (18.2%) were classified as belonging to the inflamed class. Out of these, 7 HCC carried Wnt/β-catenin mutations, and 18 HCCs did not carry Wnt/β-catenin mutations. HCCs with Wnt/β-catenin mutation were conventionally described as having an immune cold TME, which was, reportedly, attributed to the role of Wnt/β-catenin activation on the suppression of CCL5 [36]. However, in this study, we found that 17.5% (7/40) of the tumors with Wnt/β-catenin mutation had a relatively high gene expression related to $CD8^+$ T cell activation (Fig. 1) and a high expression of other immune-related molecules (Fig. 5), suggesting a subset of HCC with Wnt/β-catenin mutation in the inflamed class. Interestingly, this phenotype also showed increased expression of the genes related to DC activation including CCL4 and CCL5. This finding is also consistent with a report by Montironi et al. [16], in which the Wnt-βcatenin inflamed profile was, reportedly, characterized by upregulation of CCL4-5, CXCL9-11, genes involved in IFN-γ signature and antigen presentation. Therefore, in addition to the activation of DC, several immune steps may act in coordinate and contribute to the establishment of inflamed phenotype in this subtype of tumor [36].

We assessed whether the presence or absence of Wnt/β-catenin mutations differentially affected the characteristics of the inflamed class (Table 2): in the HCCs of the inflamed class without Wnt/β-catenin mutations, *TGFB1, SNAI3, VIM, MMP9, VEGFB, CCL4,* and *CCL5* were the most upregulated in the four groups, and indicating that they may have the most aggressive tumor traits due to the microenvironment prone to EMT and angiogenesis. This group was characterized by the most significant inhibition of the tumor suppressor gene *HNF4A* among the four groups. On the other hand, in inflamed class of HCCs with Wnt/β-catenin mutation, RNA expression of *HNF4A* is not sufficiently suppressed, and IHC often shows the expression of FOXM1, which determines aggressive tumor traits. These results suggest the possibility that, under the influence of Wnt/β-catenin signaling activation, downstream genes with distinct characteristics are both being activated.

Patients with primary liver tumors with Wnt/β-catenin inflamed profile have significantly longer RFS after liver resection (Fig. 2); 42.9% (3/7) of these patients, had non-B, non-C HCC, mainly caused by heavy alcohol consumption. The molecular characteristics were as follows: β-catenin nuclear deposition was observed in 42.9% (3/7) of cases, while GS expression was only observed in 14.3% (1/7). Although the CTNNB1 mutated region was investigated, it was poorly related to the D32-S37 mutation, which is associated with diffuse strong staining of GS [34]. One of 7 cases was positive for biliary stem cell makers, such as CK19 and EpCAM. No nodules with higher enhancement were detected in the hepatobiliary phase of Gd-EOB-DTPA-enhanced MRI. It has been shown that under the influence of Wnt/β-catenin activation signaling, HNF4A induces the bile acid transporter OATP1B3, leading to its recognition as a higher enhancement nodule in hepatobiliary phase of Gd-EOB-DTPA-enhanced MRI [15]. However, in three cases of the inflamed class that underwent MRI imaging, despite having high HNF4A expression levels ranging from 83 to

152, they did not exhibit higher enhancement HCC nodules on hepatobiliary phase of Gd-EOB-DTPA-enhanced MRI. This discrepancy significantly differs from previous reports, suggesting other signaling pathways may be affecting the expression of OATP1B3.

Previous cohorts have also reported a significantly lower postoperative recurrence rate and better survival in the inflamed class of HCC [37], and we observed the same trend in our cohort of 154 HCCs (online suppl. Fig. 1c). In 40 HCCs with Wnt/β-catenin mutations, the RFS was

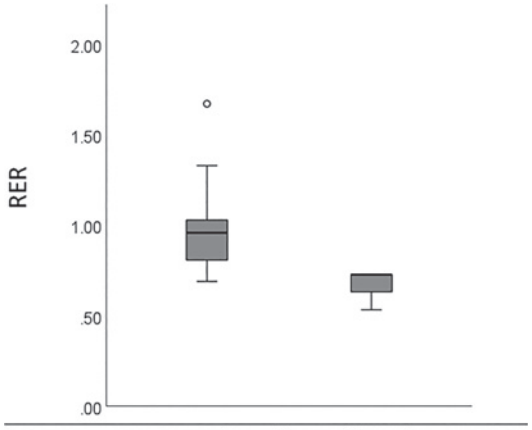

a

	non-inflamed	inflamed	P value
number	13	3	
RER average	0.99	0.66	0.065
95% C.I.	0.85 – 1.15	0.38 – 0.93	

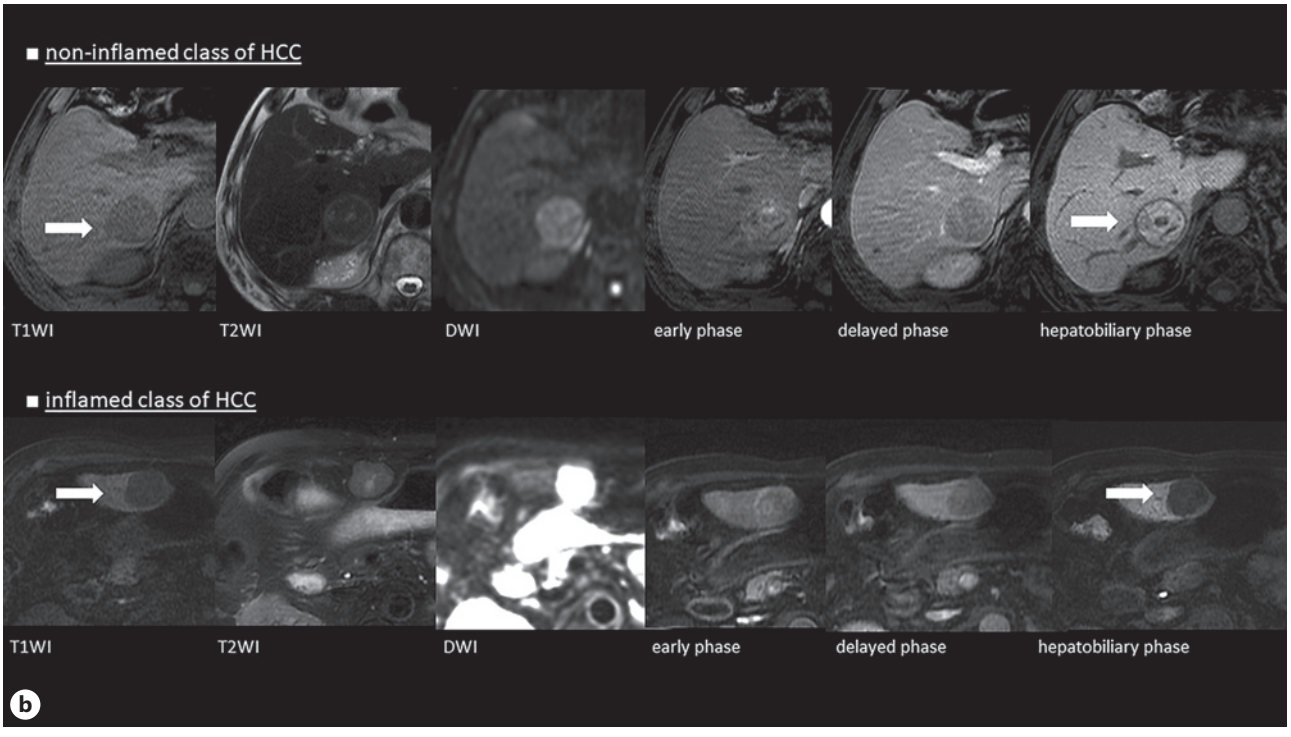

4

(Figure continued on next page.)

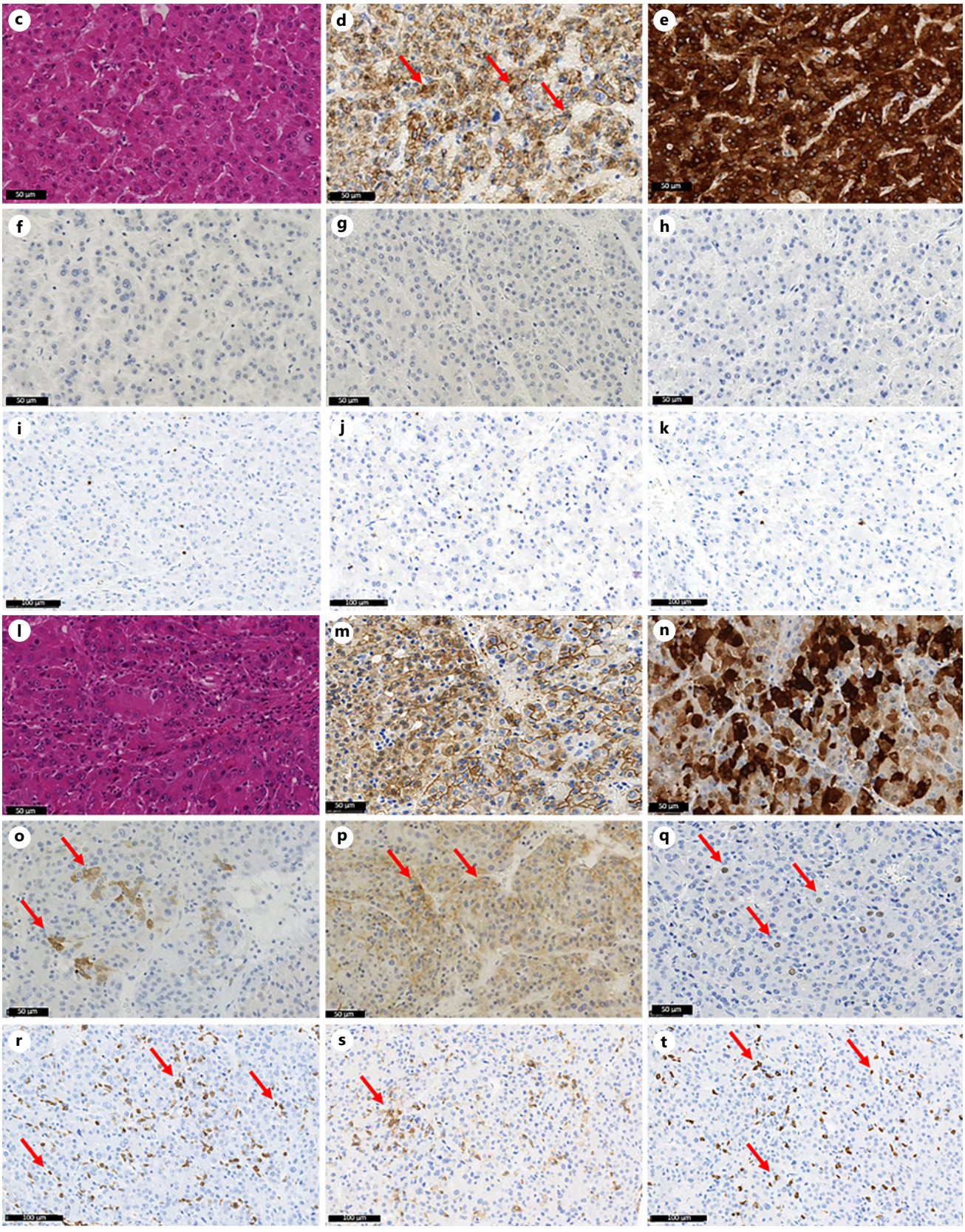

4

(For legend see next page.)

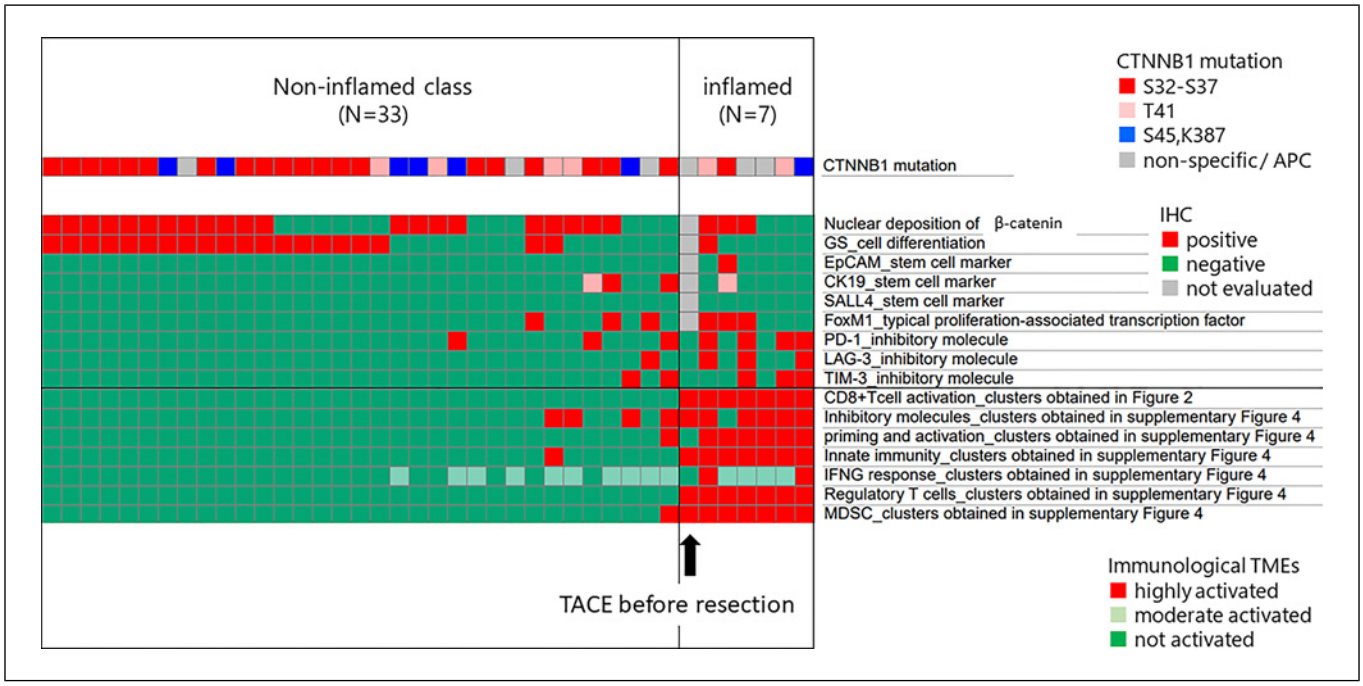

Fig. 5. Tumor immune microenvironment and immunohistochemistry results for each immune class. In HCC with Wnt/β-catenin mutations, nuclear deposition of β-catenin could be confirmed by IHC in some patients, but not in others. In the non-inflamed class, there were significantly more HCC nodules with clear GS staining (63.6% vs. 14.3%, $p = 0.047$), and most cases were negative for biliary stem cell markers such as EpCAM and CK19. Conversely, the inflamed class showed a high degree of CD8+ T-cell infiltration and expression of suppressor molecules such as PD-1, LAG-3, and TIM-3. GS was rarely stained and FOXM1-positive HCC cells were more frequently observed (see Table 2). As shown in online supplementary Figure 6, cluster analysis was performed based on gene expression levels associated with NK cells, dendritic cells, immune escape, and immunosuppressor cells (see online suppl. Table 1), and the results of these axes were described as one panel an immunological TME. In each axis, two groups were reflected in the activation and non-activation groups (three groups only for IFN-γ signaling). The non-inflamed class of Wnt/β-catenin mutated HCCs was also a non-activated group in the other axes related to tumor immunity. HCC, hepatocellular carcinoma; IHC, immunohistochemistry; FOX, forkhead box; EpCAM, anti-epithelial cell adhesion molecule; CK19, cytokeratin 19; PD-1, programmed cell death protein 1; LAG-3, lymphocyte-activation gene-3; TIM-3, T-cell immunoglobulin mucin-3; GS, glutamine synthetase; HIF, hypoxia inducible factor; NK, natural killer; TME, tumor microenvironment; IFN-γ, interferon gamma.

Fig. 4. a Differences in diagnostic imaging by immunological class – signal intensity on hepatobiliary phase of Gd-EOB-DTPA-enhanced MRI – among 40 HCC patients with Wnt/β-catenin mutations, 16 patients who underwent Gd-EOB-DTPA-enhanced MRI immediately before liver resection were included in this analysis. The non-inflamed class was recognized by the presence of higher enhancement intrahepatic nodules, which were not observed in the inflamed class. **b** Typical Gd-EOB-DTPA-enhanced MRI study of non-inflamed and inflamed class HCCs with Wnt/β-catenin mutation; (upper) image for non-inflamed class HCC. HCC nodule was recognized as a higher enhancement on hepatobiliary phase; (lower) image for inflamed class HCC. HCC nodule was recognized as a lower enhancement on hepatobiliary phase. **c–t** Typical pathological evaluations of non-inflamed and inflamed class HCC with Wnt/β-catenin mutation. Non-inflamed class of HCC were as follows: (**c**) H&E stain, moderately differentiated HCC, (**d**) β-catenin stain, nuclear deposition positive, (**e**) GS stain, positive, (**f**) CK19 stain, negative, (**g**) EpCAM stain, negative, (**h**) FOXM1 stain, negative, (**i**) CD3 staining, (**j**) CD4 staining, (**k**) CD8 staining. Inflamed class HCC were as follows: (**l**) H&E stain, moderately to poorly differentiated HCC, (**m**) β-catenin stain, nuclear deposition positive, (**n**) GS stain, negative, (**o**) CK19 stain, 1–5% positive, (**p**) EpCAM stain, positive, (**q**) FOXM1 stain, positive, (**r**) CD3 staining, (**s**) CD4 staining, (**t**) CD8 staining. The red arrows indicate positive findings. H&E, hematoxylin and eosin; HCC, hepatocellular carcinoma; GS, glutamine synthetase; CK19, cytokeratin 19; EpCAM, anti-epithelial cell adhesion molecule; FOX, forkhead box; Gd-EOB-DTPA, gadolinium-ethoxybenzyl-diethylenetriamine; MRI, magnetic resonance imaging; RER, relative enhancement ratio; CI, confidence interval.

significantly favorable in the inflamed class (Fig. 2), and similar results were confirmed through external validation using 129 HCCs with Wnt/β-catenin mutation from the TCGA database (online suppl. Fig. 3b). On the other hand, poorly differentiated HCCs with a more proliferative, stromal phenotype are known to cause vascular invasion and extrahepatic spread and have a worse prognosis. There has been no adequate validation to explain this discrepancy. Our analysis shows that the presence of Wnt/β-catenin activating mutations in the inflamed class may lead to attenuated tumor aggressiveness. We consider that this may have influenced the best RFS results in the inflamed class of HCCs with Wnt/β-catenin mutations. Additionally, there are also reports indicating better RFS in tertiary lymphoid structures formed HCCs [38]. Therefore, it is necessary to further investigate and focus on these aspects in future analyses.

Although patients with tumors with Wnt-βcatenin inflamed profile showed longer RFS, EMT-related genes, TGFβ1, and MMP9, as well as IFN-γ were significantly upregulated in this class (Fig. 3a). HCC with activated tumor immunity has a better prognosis after surgery, even with the expression of EMT-related markers. Montironi et al. [16] reported that the immune-like subgroup in the inflamed class sometimes showed Wnt/β-catenin activation, whereas TGF-β activation was a characteristic in the exhausted subgroup, where activation of Wnt/β-catenin is infrequent. Based on our analyses, the inflamed class of Wnt/β-catenin-mutated HCC shows increased expression of TGF-β, which may be related to the EMT. Because of the limited number of HCC cases with Wnt/β-catenin mutation and, reportedly, the low frequency of the immune exhausted subtype in the inflamed class, further studies involving larger cohorts are required to clarify the role of TGF-β signaling in the inflamed class of HCC with Wnt/β-catenin mutation.

Furthermore, we found that the inflamed class was characterized by abundant T-cell infiltration as well as expression of activation signals and expression of immune checkpoint molecules. Therefore, it is reasonable to hypothesize that this type of Wnt/β-catenin mutant HCC is responsive to ICI. A limitation of this cohort is that we were unable to assess the actual effectiveness of ICI in each of the four groups.

Conversely, based on the transcriptome analysis, 33 out of 40 (82.5%) HCCs with Wnt/β-catenin mutation were found to display an immune cold phenotype belonging to the non-inflamed class. Of note, 54.5% (18/33) of these HCCs were hepatitis B or C virus-induced HCCs and 90.9% (30/33) were moderately differentiated HCCs. They were also recognizable as higher enhancement intrahepatic nodules in hepatobiliary phase of the Gd-EOB-DTPA-enhanced MRI. Transcriptome analysis showed significantly lower expression of chemokines such as *CCL4, CCL5, CXCL10, CXCL11,* and *MMP9,* and high expression of GS and OATP1B3. IHC confirmed nuclear deposition of β-catenin in 63.6% (21/33) of the cases and a marker related to hepatocyte differentiation, GS, was positive in 60.0% (20/33) of the cases; only 9.1% (3/33) of the cases were positive for biliary stem cell markers. These features of the non-inflamed class well reflect the characteristics of common HCC traits with Wnt/β-catenin mutations: well to moderately differentiated HCCs (Hoshida classification S3 and Boyault classification G5/6), microtrabecular and bile plug cholestasis, high GS and high OATP1B3 expression, and can be recognized as having higher enhancement nodules in the hepatobiliary phase of Gd-EOB-DTPA-enhanced MRI. It has been demonstrated that HNF4A induces the bile acid transporter OATP1B3 in HCCs with Wnt/β-catenin activation mutations [15]. A previous report indicated that Wnt/β-catenin activating mutations generally induce low expression of CCL4 and CCL5, which results in decreased DC activation and inhibits CD8+ T cell infiltration into the tumor [36]. Based on the findings, HCCs in the non-inflamed class are likely to be resistant to ICI therapy because there are insufficient effecter cells for anti-tumor immune response [4, 7, 8].

On the other hand, collecting enough specimens for genetic analysis on unresectable HCC just prior to immunotherapy would be a difficult task. It will require thorough validation to determine how accurately the small amount of specimen collected in liver biopsy reflects the TME of the entire tumor, which may be multiple or extrahepatic spread. Our group is currently analyzing the clinical data on HCC treated with ICI, and we believe that it will be important to evaluate TME not only by liver biopsy but also by imaging diagnosis.

Phenotypic differences between HCCs with the same driver mutations, particularly Wnt/β-catenin mutations, have been reported to be defined by their profile of expression of the downstream target genes [18, 39]. Focusing on the expression of FOXM1 among Wnt/β-catenin mutated HCCs, which cooperates with canonical β-catenin to induce genes involved in the cell cycle and dedifferentiation [40], FOXM1 was positive in 9.1% (3/33) of nodules classified as non-inflamed and 42.9% (3/7) of HCCs belonging to the inflamed class. The frequencies of HCC positive for FOXM1 was significantly higher in the inflamed class than in the non-inflamed class among HCCs with Wnt/β-catenin mutation (p = 0.011). In other types of

cancer, it has been reported that stimulation from Wnt/β-catenin signaling induces nuclear migration of FOXM1; FOXM1 promotes β-catenin nuclear localization and controls Wnt target-gene expression. FOXM1 has been reported to promote the expression of c-myc and cyclin D1 and to be involved in malignant traits of tumors through dedifferentiation into cancer stem cells, promotion of EMT, and neovascularization [18]. Although FOXM1 expression in HCC has been reported to contribute to an aggressive phenotype with poor cell differentiation [15, 41], its association with Wnt/β-catenin mutations have not yet been elucidated. Future studies are required to examine the mechanism underlying the Wnt/β-catenin signaling induced expression of FOXM1 in a subset of HCC with mutation in this pathway.

One limitation of our study is the small number of cases, which included only 40 HCCs with Wnt/β-catenin mutations. As a result, we were not able to examine a matched set of background factors such as hepatitis viral infection and baseline tumor size. Therefore, the results comparing RFS and OS should be interpreted with caution. In addition, additional transcription factors may be involved in the establishment of two distinct phenotypes in HCCs with activated Wnt/β-catenin signaling.

In this study, we found that 17.5% (7/40) of HCC cases with Wnt/β-catenin mutations showed an immune phenotype characteristic for the inflamed class. This type of HCC is associated with the expression of EMT-related genes indicating that such HCC might be associated with resistance to tyrosine kinase inhibitors [42, 43]. ICIs may be effective chemotherapeutic agents because the inflamed phenotype may be responsive to ICIs. Further studies are required to clarify the efficacy of ICIs in HCC with Wnt/β-catenin mutations and T-cell-inflamed phenotype.

Conclusion

HCCs carrying mutation in Wnt/β-catenin pathway are heterogeneous population and include an inflamed class of tumors based on the transcriptome analyses and IHC. The HCC in this class shows a high degree of CD3, CD4, and CD8 positive-cell infiltration, increased expression of CCL4, CCL5, and activation of DC cells, resulting in the establishment of an immune hot TME with poor GS expression, significantly higher FOXM1 expression, and exhibiting EMT-related gene expression. Therefore, ICIs may be good chemotherapeutic agents for this class of HCCs despite the fact that these carry the activating mutation in Wnt/β-catenin pathway.

Acknowledgments

We would like to thank Editage (www.editage.com) for English language editing. We are also deeply grateful to Dr. Koji Kadota (Department of Chemistry and Biotechnology, Graduate School of Engineering, The University of Tokyo) for teaching us how to use R and R studio.

Statement of Ethics

This study was conducted in accordance with the World Medical Association Declaration of Helsinki and was approved by the Institutional Review Board of the Kindai University Hospital (approval No. #31-145). The requirement for informed consent for the academic use of archived samples for this noninvasive retrospective study was waived with an opt-out approach in the event of publication of the research plan under the Act on the Protection of Personal Information in Japan.

Conflict of Interest Statement

N.N. is an Editorial Board member of liver cancer. T.A., Y.K., K.S., M.M., H.C., M.T., S.H., H.I., K.U., Y.M. M.T., T.N., and K.N. have no relevant conflicts of interest to disclose. S.M. Michie Sakamoto is an Associate Editor of Liver Cancer. M.K. has received grants from Taiho Pharmaceuticals, Chugai Pharmaceuticals, Otsuka, Takeda, Sumitomo Dainippon-Sumitomo, Daiichi Sankyo, AbbVie, Astellas Pharma, and Bristol-Myers Squibb. M.K. has also received grants and personal lecture fees from Merck Sharpe and Dohme (M.S.D), Eisai, and Bayer, and is an adviser for MSD, Eisai, Bayer, Bristol-Myers Squibb, Eli Lilly, Chugai, AstraZeneca and ONO Pharmaceuticals. Masatoshi Kudo is an Editor-in-Chief of liver cancer.

Funding Sources

This work was supported in part by a Grant-in-Aid for Scientific Research from the Japan Society for the Promotion of Science (KAKENHI: 21K07184, N. Nishida, and 21K07950, M. Kudo) and a grant from Smoking Research Foundation (N. Nishida).

Author Contributions

Conceptualization, writing – original draft preparation, and writing – review and editing: N.N. and T.A.; methodology and project administration: N.N.; software: T.A.; validation: T.A., Y.K., and M.S.; formal analysis: K.S. and K.N.; investigation: T.A. and M.T.; data curation: T.N., K.N., K.U., M.M., H.C., M.T., S.H., H.I, and Y.M; visualization: K.S. and M.T.; supervision: M.K.

Data Availability Statement

All data generated or analyzed during this study are included in this published article and its supplementary information files. Further inquiries can be directed to the corresponding author.

References

1 Takayama T, Yamazaki S, Matsuyama Y, Midorikawa Y, Shiina S; Liver Cancer Study Group of Japan, et al. Prognostic grade for resecting hepatocellular carcinoma: multicentre retrospective study. Br J Surg. 2021 Apr 30;108(4):412–8.
2 Finn RS, Qin S, Ikeda M, Galle PR, Ducreux M, Kim TY, et al. Atezolizumab plus bevacizumab in unresectable hepatocellular carcinoma. N Engl J Med Overseas Ed. 2020 May 14;382(20):1894–905.
3 Pinyol R, Sia D, Llovet JM. Immune exclusion-wnt/CTNNB1 class predicts resistance to immunotherapies in HCC. Clin Cancer Res. 2019 Apr 1;25(7):2021–3.
4 Harding JJ, Nandakumar S, Armenia J, Khalil DN, Albano M, Ly M, et al. Prospective genotyping of hepatocellular carcinoma: clinical implications of next-generation sequencing for matching patients to targeted and immune therapies. Clin Cancer Res. 2019 Apr 1;25(7):2116–26.
5 Ruiz de Galarreta M, Bresnahan E, Molina-Sanchez P, Lindblad KE, Maier B, Sia D, et al. β-Catenin activation promotes immune escape and resistance to anti-PD-1 therapy in hepatocellular carcinoma. Cancer Discov. 2019 Aug;9(8):1124–41.
6 Chabot V, Reverdiau P, Iochmann S, Rico A, Senecal D, Goupille C, et al. CCL5-enhanced human immature dendritic cell migration through the basement membrane in vitro depends on matrix metalloproteinase-9. J Leukoc Biol. 2006 Apr;79(4):767–78.
7 Aoki T, Nishida N, Ueshima K, Morita M, Chishina H, Takita M, et al. Higher enhancement intrahepatic nodules on the hepatobiliary phase of Gd-EOB-DTPA-Enhanced MRI as a poor responsive marker of anti-PD-1/PD-L1 monotherapy for unresectable hepatocellular carcinoma. Liver Cancer. 2021 Nov;10(6):615–28.
8 Morita M, Nishida N, Sakai K, Aoki T, Chishina H, Takita M, et al. Immunological microenvironment predicts the survival of the patients with hepatocellular carcinoma treated with anti-PD-1 antibody. Liver Cancer. 2021 Jul;10(4):380–93.
9 Sasaki R, Nagata K, Fukushima M, Haraguchi M, Miuma S, Miyaaki H, et al. Evaluating the role of hepatobiliary phase of gadoxetic acid-enhanced magnetic resonance imaging in predicting treatment impact of lenvatinib and atezolizumab plus bevacizumab on unresectable hepatocellular carcinoma. Cancers. 2022 Feb 6;14(3):827.
10 Yang M, Li SN, Anjum KM, Gui LX, Zhu SS, Liu J, et al. A double-negative feedback loop between Wnt-β-catenin signaling and HNF4α regulates epithelial-mesenchymal transition in hepatocellular carcinoma. J Cell Sci. 2013 Dec 15;126(Pt 24):5692–703.
11 Colletti M, Cicchini C, Conigliaro A, Santangelo L, Alonzi T, Pasquini E, et al. Convergence of Wnt signaling on the HNF4alpha-driven transcription in controlling liver zonation. Gastroenterology. 2009 Aug;137(2):660–72.
12 Narita M, Hatano E, Arizono S, Miyagawa-Hayashino A, Isoda H, Kitamura K, et al. Expression of OATP1B3 determines uptake of Gd-EOB-DTPA in hepatocellular carcinoma. J Gastroenterol. 2009;44(7):793–8.
13 Ueno A, Masugi Y, Yamazaki K, Komuta M, Effendi K, Tanami Y, et al. OATP1B3 expression is strongly associated with Wnt/β-catenin signalling and represents the transporter of gadoxetic acid in hepatocellular carcinoma. J Hepatol. 2014 Nov;61(5):1080–7.
14 Kitao A, Matsui O, Yoneda N, Kozaka K, Kobayashi S, Koda W, et al. Gadoxetic acid-enhanced magnetic resonance imaging reflects co-activation of β-catenin and hepatocyte nuclear factor 4α in hepatocellular carcinoma. Hepatol Res. 2018 Feb;48(2):205–16.
15 Jeon Y, Kwon SM, Rhee H, Yoo JE, Chung T, Woo HG, et al. Molecular and radiopathologic spectrum between HCC and intrahepatic cholangiocarcinoma. Hepatology. 2023;77(1):92–108.
16 Montironi C, Castet F, Haber PK, Pinyol R, Torres-Martin M, Torrens L, et al. Inflamed and non-inflamed classes of HCC: a revised immunogenomic classification. Gut. 2023 Jan;72(1):129–40.
17 Kuwano A, Yada M, Narutomi F, Nagasawa S, Tanaka K, Kurosaka K, et al. Therapeutic efficacy of atezolizumab plus bevacizumab for hepatocellular carcinoma with WNT/β-catenin signal activation. Oncol Lett. 2022 Jul;24(1):216.
18 Aoki T, Nishida N, Kudo M. Clinical significance of the duality of wnt/β-catenin signaling in human hepatocellular carcinoma. Cancers. 2022 Jan 17;14(2):444.
19 Pugh RN, Murray-Lyon IM, Dawson JL, Pietroni MC, Williams R. Transection of the oesophagus for bleeding oesophageal varices. Br J Surg. 1973 Aug;60(8):646–9.
20 Marrero JA, Kulik LM, Sirlin CB, Zhu AX, Finn RS, Abecassis MM, et al. Diagnosis, staging, and management of hepatocellular carcinoma: 2018 practice guidance by the American association for the study of liver diseases. Hepatology. 2018 Aug;68(2):723–50.
21 Oken MM, Creech RH, Tormey DC, Horton J, Davis TE, McFadden ET, et al. Toxicity and response criteria of the eastern cooperative Oncology group. Am J Clin Oncol. 1982 Dec;5(6):649–56.
22 Torzilli G, Makuuchi M, Inoue K, Takayama T, Sakamoto Y, Sugawara Y, et al. No-mortality liver resection for hepatocellular carcinoma in cirrhotic and noncirrhotic patients: is there a way? A prospective analysis of our approach. Arch Surg. 1999 Sep;134(9):984–92.
23 Imamura H, Seyama Y, Kokudo N, Maema A, Sugawara Y, Sano K, et al. One thousand fifty-six hepatectomies without mortality in 8 years. Arch Surg. 2003 Nov;138(11):1198–206; discussion 1206.
24 Sim NL, Kumar P, Hu J, Henikoff S, Schneider G, Ng PC. SIFT web server: predicting effects of amino acid substitutions on proteins. Nucleic Acids Res. 2012 Jul;40(Web Server issue):W452–7.
25 Adzhubei I, Jordan DM, Sunyaev SR. Predicting functional effect of human missense mutations using PolyPhen-2. Curr Protoc Hum Genet. 2013 Jan;Chapter 7:Unit7.20.
26 Kobayashi Y, Kushihara Y, Saito N, Yamaguchi S, Kakimi K. A novel scoring method based on RNA-Seq immunograms describing individual cancer-immunity interactions. Cancer Sci. 2020 Aug 18;111(11):4031–40.
27 Newman AM, Liu CL, Green MR, Gentles AJ, Feng W, Xu Y, et al. Robust enumeration of cell subsets from tissue expression profiles. Nat Methods. 2015 May;12(5):453–7.
28 Laurent C, Charmpi K, Gravelle P, Tosolini M, Franchet C, Ysebaert L, et al. Several immune escape patterns in non-Hodgkin's lymphomas. Oncoimmunology. 2015 Aug;4(8):e1026530.
29 Tsujikawa H, Masugi Y, Yamazaki K, Itano O, Kitagawa Y, Sakamoto M. Immunohistochemical molecular analysis indicates hepatocellular carcinoma subgroups that reflect tumor aggressiveness. Hum Pathol. 2016 Apr;50:24–33.
30 Nishida N, Sakai K, Morita M, Aoki T, Takita M, Hagiwara S, et al. Association between genetic and immunological background of hepatocellular carcinoma and expression of programmed cell death-1. Liver Cancer. 2020 Aug;9(4):426–39.
31 Zhu AX, Finn RS, Edeline J, Cattan S, Ogasawara S; KEYNOTE-224 investigators, et al. Pembrolizumab in patients with advanced hepatocellular carcinoma previously treated with sorafenib (KEYNOTE-224): a non-randomised, open-label phase 2 trial. Lancet Oncol. 2018 Jul;19(7):940–52.
32 Tsuboyama T, Onishi H, Kim T, Akita H, Hori M, Tatsumi M, et al. Hepatocellular carcinoma: hepatocyte-selective enhancement at gadoxetic acid-enhanced MR imaging--correlation with expression of sinusoidal and canalicular transporters and bile accumulation. Radiology. 2010 Jun;255(3):824–33.
33 Sia D, Jiao Y, Martinez-Quetglas I, Kuchuk O, Villacorta-Martin C, Castro de Moura M, et al. Identification of an immune-specific class of hepatocellular carcinoma, based on molecular features. Gastroenterology. 2017 Sep;153(3):812–26.
34 Rebouissou S, Franconi A, Calderaro J, Letouze E, Imbeaud S, Pilati C, et al. Genotype-phenotype correlation of CTNNB1 mutations reveals different ß-catenin activity associated with liver tumor progression. Hepatology. 2016 Dec;64(6):2047–61.
35 Hsu CL, Ou DL, Bai LY, Chen CW, Lin L, Huang SF, et al. Exploring markers of exhausted CD8 T cells to predict response to immune checkpoint inhibitor therapy for hepatocellular carcinoma. Liver Cancer. 2021 Jul;10(4):346–59.

36 Kudo M. Gd-EOB-DTPA-MRI could predict WNT/β-Catenin mutation and resistance to immune checkpoint inhibitor therapy in hepatocellular carcinoma. Liver Cancer. 2020 Sep;9(5):479–90.
37 Schoenberg MB, Li X, Li X, Han Y, Hao J, Miksch RC, et al. The predictive value of tumor infiltrating leukocytes in Hepatocellular Carcinoma: a systematic review and meta-analysis. Eur J Surg Oncol. 2021 Oct; 47(10):2561–70.
38 Li J, Nie Y, Jia W, Wu W, Song W, Li Y. Effect of tertiary lymphoid structures on prognosis of patients with hepatocellular carcinoma and preliminary exploration of its formation mechanism. Cancers. 2022 Oct 21;14(20): 5157.
39 Clevers H. Wnt/β-Catenin signaling in development and disease. Cell. 2006 Nov 3; 127(3):469–80.
40 Raychaudhuri P, Park HJ. FoxM1: a master regulator of tumor metastasis. Cancer Res. 2011 Jul 1;71(13):4329–33.
41 Yamashita T, Kitao A, Matsui O, Hayashi T, Nio K, Kondo M, et al. Gd-EOB-DTPA-enhanced magnetic resonance imaging and alpha-fetoprotein predict prognosis of early-stage hepatocellular carcinoma. Hepatology. 2014 Nov;60(5):1674–85.
42 Mir N, Jayachandran A, Dhungel B, Shrestha R, Steel JC. Epithelial-to-Mesenchymal transition: a mediator of sorafenib resistance in advanced hepatocellular carcinoma. Curr Cancer Drug Targets. 2017;17(8):698–706.
43 Xia S, Pan Y, Liang Y, Xu J, Cai X. The microenvironmental and metabolic aspects of sorafenib resistance in hepatocellular carcinoma. EBioMedicine. 2020 Jan;51: 102610.